ผลของอัตราส่วนความดันย่อยของออกซิเจนต่อโพรเพนและอุณหภูมิ ต่อการปรับปรุง
ความว่องไวของตัวเร่งปฏิกิริยาทางไฟฟ้าเคมีที่ไม่เป็นไปตามกฎของฟาราเดย์
ของการออกซิเดชันโพรเพนบนแพลตินัมบนอิตเทรียสเตบิไลซ์เซอร์โคเนีย

นางสาวสรีรัตน์ ทองศรีเกตุ

วิทยานิพนธ์นี้เป็นส่วนหนึ่งของการศึกษาตามหลักสูตรปริญญาวิศวกรรมศาสตรมหาบัณฑิต
สาขาวิชาวิศวกรรมเคมี ภาควิชาวิศวกรรมเคมี
คณะวิศวกรรมศาสตร์ จุฬาลงกรณ์มหาวิทยาลัย
ปีการศึกษา 2560

Effects of ratio of oxygen partial pressure to propane partial pressure and temperature on non-faradaic electrochemical modification of catalytic activity (NEMCA) of propane oxidation on Pt-YSZ

Miss Sareerat Thongsrigate

A Thesis Submitted in Partial Fulfillment of the Requirements
for the Degree of Master of Engineering Program in Chemical Engineering
Department of Chemical Engineering
Faculty of Engineering
Chulalongkorn University
Academic Year 2017

Thesis Title	Effects of ratio of oxygen partial pressure to propane partial pressure and temperature on non-faradaic electrochemical modification of catalytic activity (NEMCA) of propane oxidation on Pt-YSZ
By	Miss Sareerat Thongsrigate
Field of Study	Chemical Engineering
Thesis Advisor	Palang Bumroongsakulsawat, Ph.D.

Accepted by the Faculty of Engineering, Chulalongkorn University in Partial Fulfillment of the Requirements for the Master's Degree

.....Dean of the Faculty of Engineering

(Associate ProfessorSupot Teachavorasinskun, D.Eng.)

THESIS COMMITTEE

.....Chairman

(ProfessorSuttichai Assabumrungrat, Ph.D.)

.....Thesis Advisor

(Palang Bumroongsakulsawat, Ph.D.)

.....Examiner

(Akawat Sirisuk, Ph.D.)

.....External Examiner

(Suwimol Wongsakulphasatch, Ph.D.)

CONTENTS

Page

Page

LIST OF FIGURES

Page

LIST OF TABLES

Page

CHAPTER I
INTRODUCTION

1.1 Background

Automotive exhaust gases from engines contain harmful compounds. As a result of incomplete combustion, exhaust gases include carbon monoxide (CO) and hydrocarbons (HC). Catalytic purification can be used to reduce their emissions in exhaust gases. Most of automobiles are supplied with catalyst converters for the removal of major pollutants such as CO, NOX and HC. The exhaust gas purification system currently in use consists of a catalytic converter and an air (oxygen)/fuel ratio controller [1].

The catalysts used in the converters are mostly precious metals such as platinum, palladium and rhodium. Platinum is considered the most active metal for the oxidation of hydrocarbons [2, 3]. So it has been used in catalytic converters for oxidation of residual fuels. Currently, because of the rising prices of precious metals, catalyst consumption should be more efficient. The Non-faradaic electrochemical modification of catalytic activity (NEMCA) effect or the electrochemical promotion of catalysis of catalyst, which could increase catalytic oxidation rates of hydrocarbons, could be used to shorten the length of catalytic converters and thereby to reduce catalyst consumption. This research studies the NEMCA effect with cells prepared by sputtering for the oxidation of propane as a model reaction of the oxidation of residual light hydrocarbons. The effect of the partial pressure ratio of oxygen and propane, temperature and potential differences on NEMCA performance will be studied.

1.2 Research objectives

1. To observe the electrochemical promotion of catalysis for propane oxidation on Pt-YSZ cells in wireless and conventional configuration.

2. To study the effects of temperature and applied potentials on propane oxidation reaction for wireless configuration.

3. To study the effects of different partial pressure of oxygen, temperature and applied potentials on propane oxidation reaction for conventional configuration.

1.3 Research scopes

1.3.1 Wireless configuration

1. Effect of the preparation methods and Pt loading, i.e. wet impregnation and sputtering coat methods.

2. Effect of the temperature range 200-500 ℃ on NEMCA performance.

3. Effect of potential differences from 0 to 30 V on NEMCA performance.

1.3.2 Conventional configuration

1. Effect of the partial pressure oxygen on sputtered Pt film on YSZ on NEMCA performance.

2. Effect of the temperature range 200-500 ℃ on NEMCA performance.

3. Effect of potential differences from -1 to +1 V on NEMCA performance.

4. Reactants feed compositions at 3% propane and 10% oxygen balance helium

CHAPTER II
THEORY AND LITERATURE REVIEW

2.1 Impregnation

Impregnation is among the simplest, least expensive and most regular methods to prepare supported metal catalysts. A high surface area oxide or carbon support is contacted with liquid solutions to deposit dissolved metal ions or metal precursors [4].

The first requirement can be reached by dissolving the precursor in a liquid. The former step of the metal complex is called impregnation. After impregnation, wet slurry of metal precursor and support are dried. And then they are heated in order to remove the ligands known as calcination and to reduce the metal to active element state. The calcination is a system in which the solid/gas interface replaces the solid/liquid interface [5]. Catalyst synthesis steps are extended in Figure 2.1.

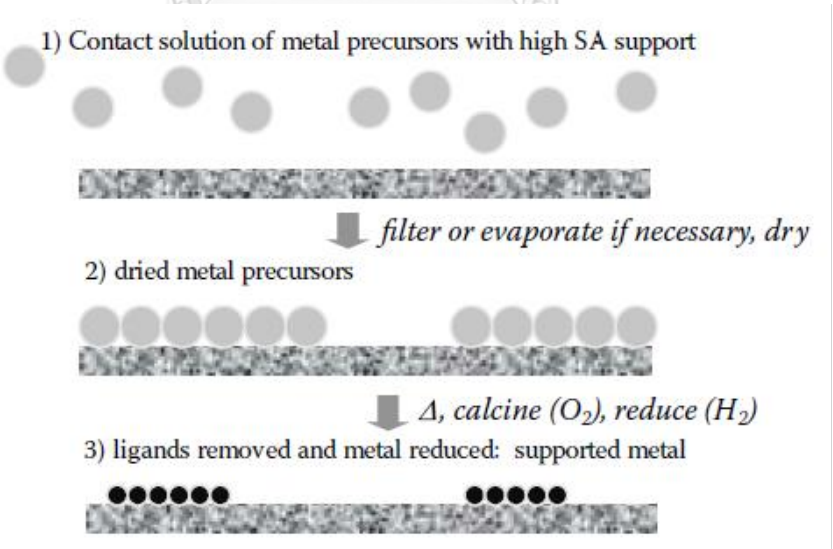

Figure 2.1 Stages of catalyst preparation by aqueous impregnation [4].

2.2 Sputtering

Sputter deposition is a widely used technique to deposit thin films on substrates. This technique is based upon ion attack of the target material. Ion attack results in a vapor due to a purely physical process, i.e. the sputtering of the target material. Hence, this technique is part of the class of physical vapor deposition techniques. The most common approach for growing thin films by sputter deposition is the use of a magnetron source in which positive ions present in the plasma of a magnetically enhanced glow discharge attack the target. The target can be powered in different ways, ranging from DC for conductive targets, to RF for nonconductive targets, to a variety of different ways of applying current and/or voltage pulses to the target. To model this behavior, the fluxes of the various species to the target must be determined. The fluxes of species incident at the substrate are important because they not only influence the reactive sputter deposition process, but also control the growth of the required film. Certainly, the microstructure of magnetron sputter deposited films is defined by the identity of the particles arriving at the substrate, their fluxes and the energy per particle [6].

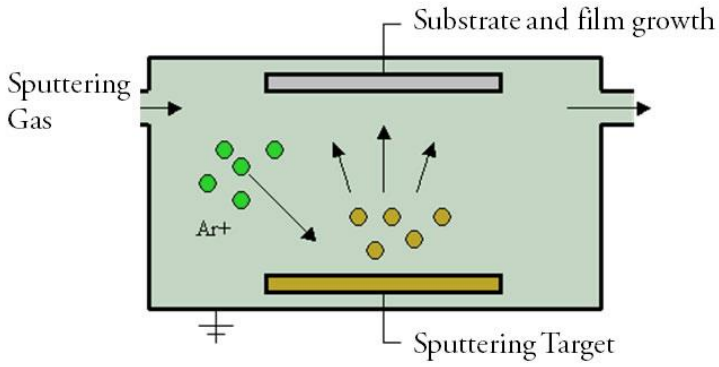

Figure 2.2 Sputter deposition process [7].

Argon gas is ionized and accelerated to a target (Figure 2.2). The argon ions impact the target causing ejection of the target material, which will coat the substrate [7].

There are several methods for preparation of the Pt-YSZ composites, such as impregnation method [8], sol-gel method [9, 10], gas phase deposition (spray pyrolysis deposition) [11], sputtering method [12, 13], coating method [14], and carbon-incorporated [15]. Table 2.1 is a summary of the reports about the preparation of Pt-YSZ composites. In this work [13], sputter-deposited films of Pt with a thickness of 60 nm are interfaced with YSZ investigated on the propane combustion. Catalytic performances were compared with Pt-paste films catalysts. Sputtered catalysts presented higher Pt dispersion and larger catalytic activity. The magnitude of the electrochemical activation was higher for sputtered electrochemical catalysts than for Pt-paste films.

These studies concerned about influence of the thickness of sputter-deposited Pt films on the NEMCA effect of hydrocabons combustion [16-18]. 8 to 120 nm-thick Pt coatings were sputtered on YSZ of propane combustion which can observe the better performance for 60 nm-thick Pt coating (Λ = 1980) than that for the thinner (Λ = 1040) or for the thicker (Λ = 1600) [16]. The catalytic reaction of ethylene combustion on porous Pt paste-deposited on YSZ, as expected from the O^{2-} reaction-diffusion model of electrochemical promotion, the catalytic rate enhancement ρ decrease and the Faradaic efficiency Λ increase moderately with increasing film thickness, since the surface concentration of O^{2-} near the gas-exposed top of the Pt film decreases significantly due to the reaction with ethylene [17, 18].

Table 2.1 Comparison the preparation method of the Pt-YSZ composites.

Preparation method	Precursors	Average diameter		Determination	Reference
		Pt	YSZ		
Impregnation method	H_2PtCl_6, YSZ powder	~50 nm	-	TEM	[8]
Sol-gel method	$PtCl_4$, $Y(NO_3)_3$, $ZrOCl_2$	~100 nm	~100	SEM	[9]
Sol-gel method	Zirconium tetra-n-butoxide, $Y(NO_3)_3$, Pt salt	< 50 nm	< 50 nm	FE-SEM	[10]
Spray pyrolysis deposition	$Y(NO_3)_3$, $ZrCl_4$, $H_2[PtCl_6]$	~40 nm	17-24	XRD	[11]
Sputtering method	YSZ pellet, Pt	-	-	-	[12]
Sputtering method	YSZ pellet, Pt	-	-	SEM	[13]
Coating method	YSZ disc, Pt	-	-	SEM	[14]
Carbon-incorporated	H_2PtCl_6, $Y(NO_3)_3$, $ZrO(NO_3)_2$	25-35 nm	5-10 nm	TEM	[15]

- : unreported

2.3 Catalytic converter

The exhaust gas purification system consists of a catalytic converter and an electronically controlled air/fuel management system. The air inlet and fuel injection are controlled to provide a stoichiometric ratio between oxygen (air) and fuel. The objective is to keep the air-to-fuel ratio (A/F-ratio) within the narrow range as presented in figure 2.3. In this lambda window, the high conversions (>80-90%) of CO, HC and NO_X are achieved simultaneously. If the A/F-ratio is below 14.6, the exhaust gas contains more reducing reactants (CO, HC) than oxidizing reactants (O_2, NO_X) and the engine operates under rich conditions. If the A/F-ratio exceeds 14.6, the engine operates under lean conditions. [1]

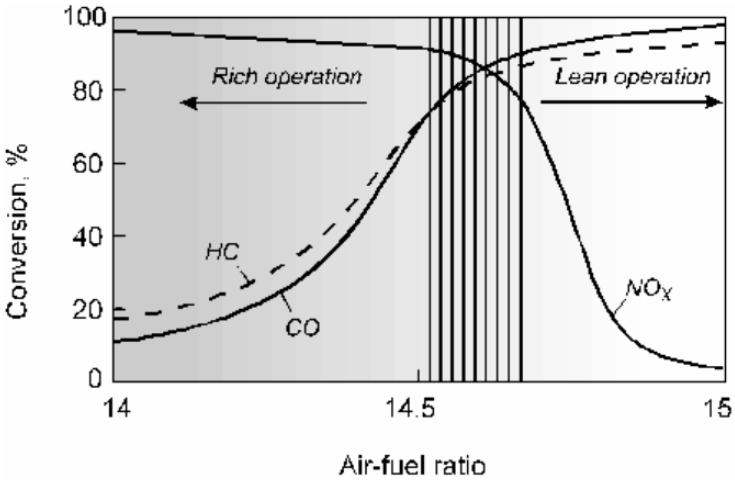

Figure 2.3 The conversion efficiency (%) of a three-way catalyst as a function of A/F-ratio. The lambda window, an A/F-ratio of 14.6 corresponds to stoichiometric operation, λ=1 [1]

2.3.1 Structure of a three-way catalyst

Three-way catalysts have a honeycomb-like, monolithic structure. The monolith support is made either from metallic or ceramic material. The monolith contains small channels about 300-600 channels per square inch. The washcoat, which includes the active catalyst material, is impregnated on channel walls. The washcoat consists of porous oxides, such as γ-Al2O3 and precious metals. The thickness of the washcoat layer is circa 20-60 μm and it has a large surface area of approximately 50-200 m^2/g. Thus the diffusional resistance is minimal and gases easily reach the active surface sites, which allows close to 100% conversion with a high catalytic activity. The use of a layered washcoat has been applied in commercial three-way catalysts. The main compounds in the washcoat are base-metal oxides, such as aluminium, cerium and zirconium. In addition, the CaO and MgO compounds are used as additives in the washcoat to promote the catalytic activity or to stabilise the structure of the catalyst. The precious metals currently used in three-way catalyst applications are platinum, palladium and rhodium. These metals are well-known catalysts with high activities for controlling the exhaust emissions, and they are also preferred because they are less inclined to poisoning compared to metal oxide catalysts, such as CuO. The amount of the active metals in the catalyst is normally circa 1-2 wt-% of the washcoat. Precious metals are used to reduce the emissions of exhaust gases of reducing or oxidizing agents, such as hydrocarbons, CO and hydrogen, and oxygen and NO_X respectively. Rhodium is used to be an efficient catalyst for NO_X reduction, whereas palladium and platinum metals are used in CO and hydrocarbon oxidation reactions, in especially during cold start. Therefore, commercially-used three-way catalysts for gasoline engines are often a bimetallic combination of the precious metals, such as Pt-Rh or Pd-Rh. [1]

2.3.2 Phenomena in the three-way catalyst operation

The performance of a three-way catalyst depends on the factors including, for example, the chemistry (such as the preparation, materials and loadings) and the physics (such as the support and converter design) of the catalyst, and the chemical engineering aspects such as the gas composition, reaction temperatures and dynamic conditions. Three-way catalysts operate under dynamic and fluctuating conditions. The catalytic reactions occur at normal exhaust gas temperatures which can vary from 300°C to 400°C, even up to about 1000°–1100°C, depending on the driving conditions. High operation temperatures should be avoided in order to prevent sintering of the precious metals and washcoat compounds. There are also temperatures and concentration gradients present in the catalytic converter, and the space velocity of the gas flow and the exhaust gas composition fluctuate as well. Therefore, catalysts have to be thermally and mechanically stable against the physical and chemical changes to avoid deactivation. [1]

2.4 NEMCA

The heterogeneous catalytic process can be activated and promoted by electrochemistry which does not follow Faraday's law. It was reported that the catalytic activity and selectivity of catalyst deposited on solid electrolytes could be modified by applying potentials between the working electrode (catalyst) and the counter electrode (second electronic conductor). Both of these electrodes deposited on the solid electrolyte. The electrochemically induced catalytic rate increases to 200 times which was larger than the catalytic rate excluding current application [19]. The electrochemical (electrocatalytic) oxidation rate in Faraday's law equals I/nF , where I is the applied current, n is the charge of the ion supplied to the catalyst via the solid electrolyte, and F is Faraday's constant. So the rate increase is strongly non-faradaic and exceeds the steady-state rate increase. The Faradaic efficiency (**Λ**) of the process also increases. This effect is called non-faradaic electrochemical modification of catalytic activity (NEMCA effect). It is used for describing the electrochemical activation of heterogeneous catalysis.

According to the typical NEMCA experiment, the reactants such as C_2H_4 and O_2 are co-fed over a conductive catalyst which is used as the working electrode on a solid electrolyte cell. [19]

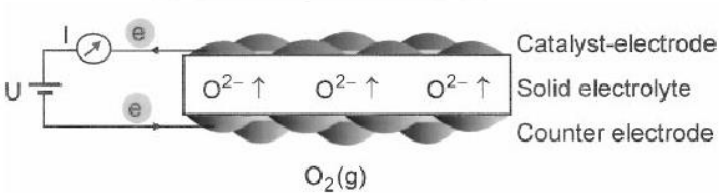

Figure 2.4 Experimental setup used in NEMCA experiments. [19, 20]

Figure 2.4 shows the experimental setup of varying the potential of the catalyst/working electrode. The cell current (I) is also varied. The electrocatalytic reactions taking place at the catalyst/solid electrolyte/gas three-phase-boundaries (tpb), are:

$$O^{2-}\ (YSZ) \longrightarrow O(a) + 2e^{-} \qquad (1)$$

$$C_3H_8 + 10O^{2-}(YSZ) \longrightarrow 3CO_2 + 4H_2O + 20e^{-} \qquad (2)$$

O(a) means atomic oxygen which is adsorbed on catalyst surface. The current changes along with the change of potential which affects the electrocatalytic rate reaction. The catalytic rate of the catalytic (no net charge-transfer) reaction is:

$$C_3H_8 + 5O_2 \longrightarrow 3CO_2 + 4H_2O \qquad (3)$$

The electrocatalytic reactions taking place on the metal catalyst (working electrode) will change at the same time. So each ion supplied by the solid electrolyte to the catalyst can cause many gaseous molecules to react catalytically. Thus, in the case of YSZ solid electrolyte might be expected that the O^{2-} ions supplied to catalyst would cause a catalytic rate increase (if all O^{2-} supplied to the catalyst were reacting with C_3H_8 forming CO_2 and H_2O).

The oxygen chemical potential difference which is a driving force for oxygen ions to migrate across the electrolyte and to backspillover onto the catalyst surface is proved. The reaction is promoted in agreement with electrochemical promotion of catalysis rules by the formation of a double layer of oxide ions on the catalyst surface. The cathodic reduction of solid electrolyte cells utilizing YSZ (O^{2-} pumping) is:

$$1/2O_2\,(g) + 2e^- \overset{Pt}{\longleftrightarrow} O^{2-}\,(YSZ) \qquad (4)$$

The NEMCA effect can be explained in Figure 2.4. Ions have been arrived under the influence of the applied current or potential at the three-phase boundaries including catalyst/solid, electrolyte, and gas from the adsorbed species O(a). The adsorption of species O(a) have only three possibilities including:

(a) Desorption to the gas phase

(b) Reaction with a coadsorbed species

(c) Migration over the entire gas-exposed catalyst electrode surface (spillover) followed by possible desorption or reaction with coadsorbed species

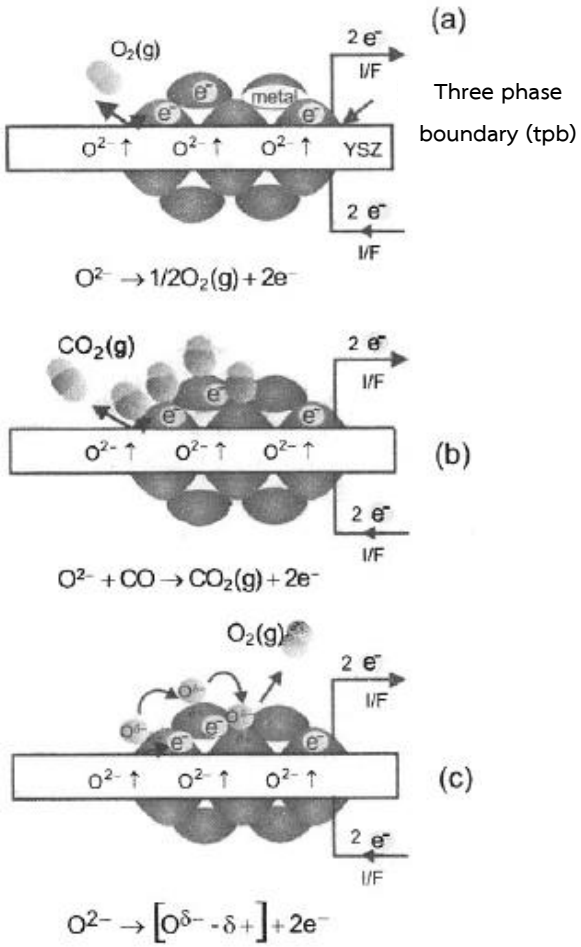

Figure 2.5 Possible pathways of O(a) adsorbed species created at three-phase boundaries via application of electric current: (a) Desorption; (b) Reaction; (c) Backspillover. [19]

In case 2.5(a), the rate (r) of the catalytic reaction (e.g. CO oxidation) will not be affected but in case 2.5(b), the rate increase (Δr) will equal I/nF (e.g. reaction of O^{2-} with CO).

In case 2.5(c), however, the new species is generated onto the catalyst surface. And the product remains on the catalyst surface and changes the catalytic or promotional properties. Thus, NEMCA occurs in this case.

The effect of electrochemical promotion (EP), or in situ controlled promotion (SCP), or NEMCA, is caused by an electrochemically controlled migration (backspillover) of O^{2-} ion from the solid electrolyte onto the gas phase. It results in

activated surface of metal electrodes. These ions charge in the metal form an effective electrochemical double layer on the gas-phase catalyst surface shown in Figure 2.6. And these ions change their work function and effect of the catalytic phenomena about the reversibility and the operation. [19]

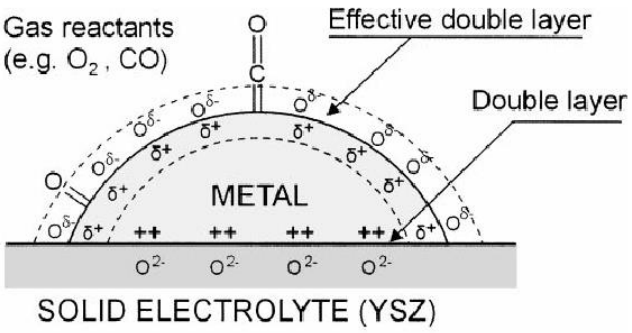

Figure 2.6 Schematic representation of a metal electrode deposited on a O^{2-} - conducting showing the location of the metal electrode double layer, the effective double layer, and the effective double layer created at the metal/gas interface due to potential-controlled ion migration (backspillover). [19, 20]

The application of electropromotion of the catalytic oxidation of hydrocarbons has received considerable attention. The catalyst combustion are mainly support noble metals such as Pt and Pd. Pd has been used in the case of methane oxidation [21-25], However, Pt is considered the most active metal for the oxidation of hydrocarbons [2, 3].

The propane oxidation on Pt-YSZ have been researched and the works are shown in Table 2.2 which summarizes the catalytic system using oxygen ion (O^{2-}) conductor supports [2, 3, 12-14, 26-29]. The Pt catalyst-electrodes deposited on YSZ are among the most widely studied systems, and rate enhancement ratio as high as 1,450 [2], 1,400 [3], and 1,350 [14, 27] have been found. From Table 2.2, the mode of metal film preparation strongly affects the maximum ρ values. Apart from the oxidation of hydrocarbons [30-32], CO oxidation [33, 34], and NO oxidation [35] could also be observed with the NEMCA effect.

Table 2.2 Propane oxidation of metal supported on oxygen ionic conducting support.

Catalyst (W)	Solid electrolyte	C & R Electrode	Reactants (O_2, C_3H_8)	T (^{o}C)	ρ_{max} (>1)	Rate behavior	Special feature	Ref.
Pt	YSZ	Ag	PO_2/PC_3H_8= 0.5-2.2	300-500	1450 (Pt)	Inverted volcano	Oscillatory behavior [2], Comparison to Pd, Ag on YSZ, Reaction of Pt exhibited a strong NEMCA effect.	[2, 3, 26]
Pt	YSZ	Au	PO_2= 0-3 kPa PC_3H_8= 0-6 kPa	420-520	1350 (Pt) 6 (Rh)	Inverted volcano	Comparison to Rh on YSZ.	[14]
Pt	YSZ	Au	PO_2/PC_3H_8= 0.5, 3.4	425-520	1350 (Pt) 4 (Rh)	Inverted volcano	Comparison to Rh on YSZ	[27]
Pt	YSZ	Au	$[C_3H_8]/[O_2]$ = 2300 ppm	150-500	22.4 (sputter) 1.4 (paste)	Electrophobic	Pt nanometric, Comparison to sputtered-film and paste film.	[13]
Pt	YSZ	Au	$[C_3H_8]/[O_2]$ = 1000 ppm	350	-	Electroph obic	Isotropic lebeling	[28]
Pt	YSZ pellet	Au	PO_2= 4.5 kPa PC_3H_8= 0.2 kPa	350	-	Electrophobic	Permanent EPOC γ=1.3	[12]
Pt	YSZ	Ag	$[C_3H_8]/[O_2]$ = 8000 ppm $[C_3H_6]/[O_2]$ = 7710 ppm	170	-	Electrophobic	Comparison to propane And propene oxidation	[29]

- : unreported, W : working , C : counter, R : reference

The mathematical model of promotion is in qualitative agreement with the experiment. Figure 2.7 describes all electrochemical promotion classified to four main types including electrophobic, electrophilic, volcano, and inverted volcano [19].

In figure 2.7 (a), it is strong adsorption of the electron acceptor and weak adsorption of the electron donor. This leads to electrophobic behavior. In figure 2.7 (b), it is strong adsorption of the electron donor and weak adsorption of the electron acceptor. This leads to electrophilic behavior. In figure 2.7 (c), it is strong adsorption of both the electron donor and electron acceptor. This leads to volcano behavior. And figure 2.7 (d) is the case of weak adsorption of both the electron donor and electron acceptor. This leads to inverted volcano behavior.

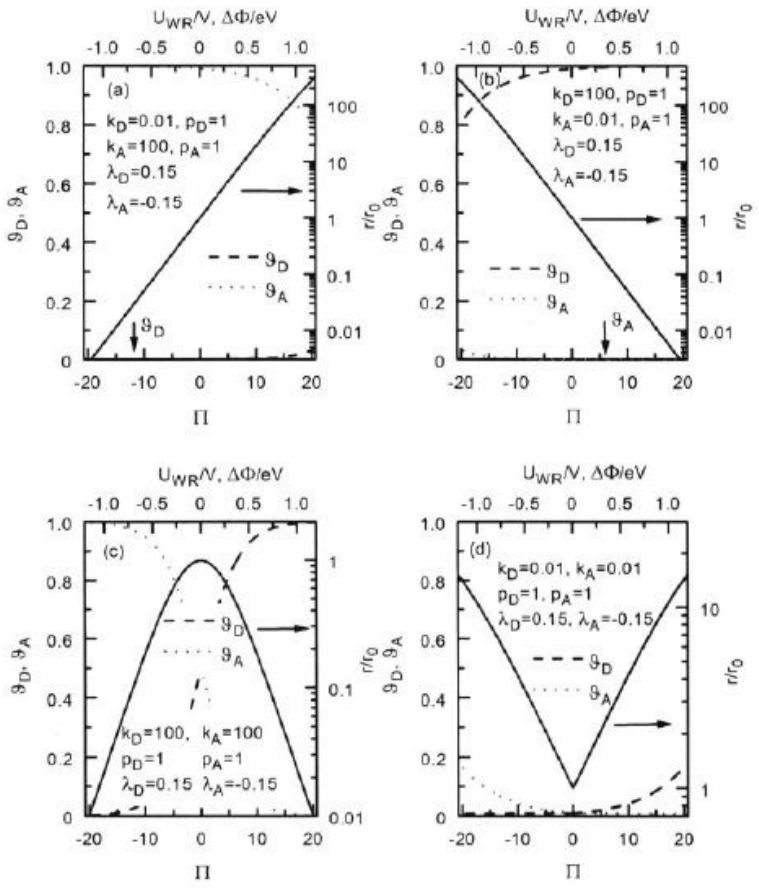

Figure 2.7 Model predicted the four types electrochemical promotion behavior: (a) electrophobic, (b) electrophilic, (c) volcano-type, and (d) inverted volcano-type [19, 36].

The phenomenon type of the reactions is able to exhibit more than one type depends on the reaction conditions and properties of catalyst. Propane oxidation of Pt-YSZ, for example, at low propane concentration [29], it exhibited electrophobic behavior but exhibited inverted volcano behavior at high propane concentration [26].

The examples of effect of catalyst potential U_{WR}, work function, current, and dimensionless catalyst potential $\Pi = F\Delta U_{WR}/RT$ on the rates such as Oxidation of CH_4 on Pt film deposited on YSZ for high CH_4/O_2 feed ratios (20:1 and 40:1), NO reduction by C_2H_4 on Pt film deposited on YSZ, CO oxidation on Pt film deposited on YSZ, and CH_3OH oxidative dehydrogenation to H_2CO on Pt film deposited on YSZ have been respectively shown in Figure 2.8(a) – 2.8(d) [19, 20].

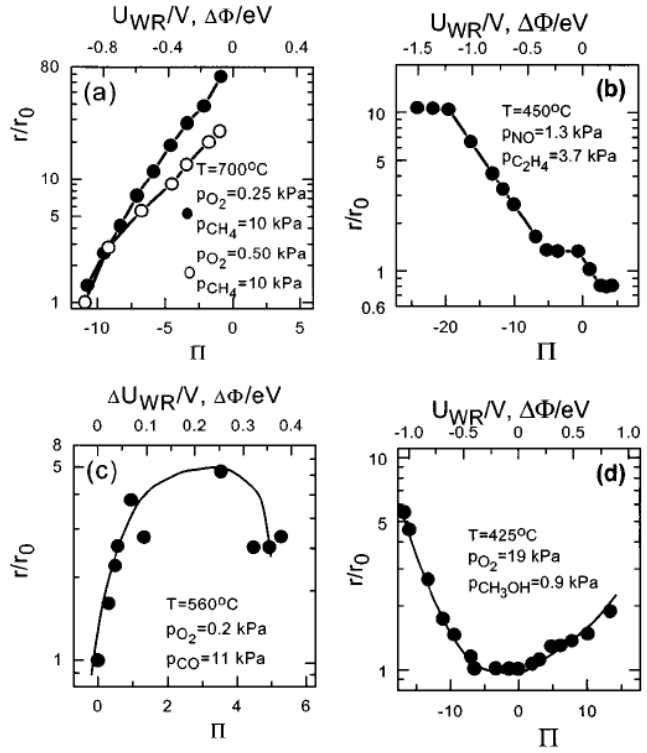

Figure 2.8 Example of the four types of electrochemical promotion behavior: (a) electrophobic, (b) electrophilic, (c) volcano-type, and (d) inverted volcano-type [19, 20].

2.5 Reactor configuration

The conventional configuration is shown in Figure 2.9 (a), which is directly electrical connected of catalyst to power supply. The Pt catalyst is used as the working electrode and Au is used as the counter electrode. The polarization is applied between Au and Pt electrodes which used as cathode and anode.

Figure 2.9 (b) shows the bipolar configuration. In their system, a Pt stripe was deposited between two gold electrodes onto YSZ dick (Figure 2.10). In this configuration, the film of catalyst is not directly polarized. Part of the catalytic material is polarized with a positive charge, while the other part is polarized with a negative charge. One part of the catalyst acts as an anode and the other as a cathode. There is no uniform catalyst where Pt is used as a working electrode. The increase in the catalytic activity is the result of the negative and positive polarization of the catalytic material. Therefore, reactions that exhibit both electrophobic and electrophilic behavior are the more suitable to be used in this kind of bipolar configurations. The catalytic combustion on the Pt stripe can be electropromoted by applying a current between the two gold electrodes. [45]

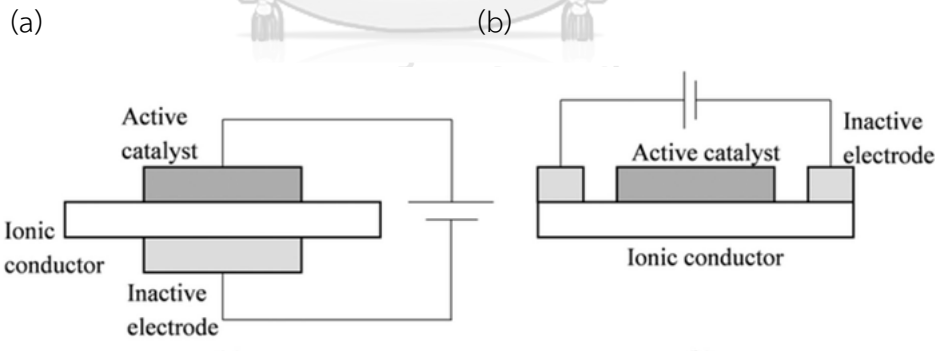

Figure 2.9 Electrode geometry in (a) conventional NEMCA configuration and (b) wireless configuration (non-direct polarizations)

The bipolar configuration of the electrochemical catalyst shown in figure 2.10 was the first significant development. A bipolar configuration allows the polarization of the catalytic layer without any direct electrical connection (Figure 2.10) [37]. For

example, Pt stripes were deposited between two gold electrodes on the same side of a YSZ disk. The rate of the ethylene catalytic combustion on the Pt stripe can be electropromoted by applying a current between the two gold electrodes [38, 39].

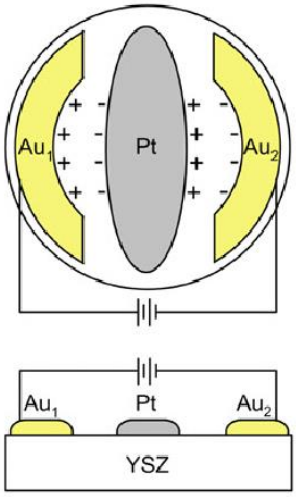

Figure 2.10 Configuration and dimensions of the bipolar cell [37].

For example of the wireless bipolar cases (Figure 2.11), the reduction of NO by CO or C_3H_6 in the presence of O_2 was investigated on porous polycrystalline Rh catalyst films using a single-chamber and a wireless bipolar cell configuration. In the latter case the Rh catalyst films were deposited on the inner side of a YSZ tube, while two Au films deposited on the outer side of the tubes were used to polarize the Rh catalyst surface. It was found that both direct (conventional) and indirect (wireless) polarization of the catalyst causes significant enhancement in the reaction rates (up to a factor of 20) and in the reactant conversion. These rate increases are strongly NEMCA [40].

This research describes the result of using of the NEMCA effect or Electrochemical Promotion (EP). The following system is C_2H_4 oxidation on electronically isolated Pt catalysts on YSZ where NEMCA is induced via potential application between two terminal Au electrodes also supported on the solid electrolyte (wireless configuration) [39].

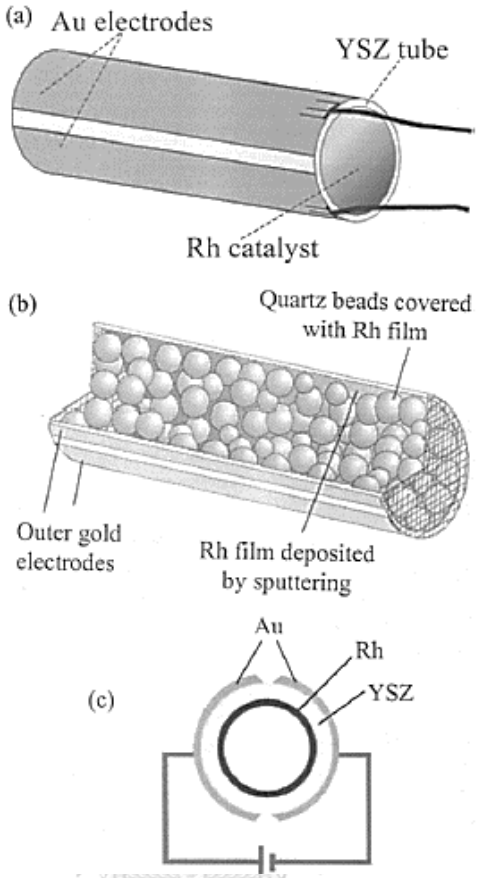

Figure 2.11 A schematic of non-conventional bipolar tube reactor configurations: empty (a) and filled with Rh-coated glass beads (b) YSZ tubes where catalyst is deposited on the inner wall and two gold electrodes are deposited on the outer wall. These designs do not need direct electrical connection to the catalyst-working electrode (bipolar design) as shown in (c) [40].

The study of Poulidi, D. and co-worker, the results on the modification of a platinum catalyst film supported on a pellet of SCYb, considered being a mixed protonic–electronic conductor under reducing conditions. The wireless configuration is applied to the mixed ionic and electronic conductivity of the supporting membrane to supply an ionic promoting species to the catalyst surface. Controlling the flow of this species is achieved by adjusting the effective hydrogen chemical potential difference across the membrane in a dual-chamber reactor [41].

In this research [42], they study the effect of macroscopically applied oxygen chemical potential differences to a platinum catalyst supported on a mixed oxygen ion and electronic conducting membrane. It is found that the oxygen chemical potential difference causes the back-spillover of oxygen species from the support onto the catalyst surface, resulting in the modification of the catalytic activity.

2.6 Platinum

Pt is a silver-gray, lustrous, malleable, and ductile metal. The structure of Pt at ambient is face-centered cubic. The platinum compounds are mainly found in oxidation states +2 and +4 in addition +1, +5 and +6. Some physical and chemical properties are shown in Table 2.3. Tetravalent platinum compounds are soluble in water except for platinic oxide [43].

Table 2.3 The physical and chemical properties of Platinum.

Properties	Value
Atomic mass	195.078
Atomic number	78
Density	21.447 g/cm^3
Melting point	1,773.5 $\pm$ 1 ^{o}C
Boiling point	3,827 ^{o}C (approximated)

The major industrial users of Pt are the automotive, electronic, chemical, jewelry, dental, and glass industries. Pt has extensive catalytic qualities. For example, it is used in catalytic converters in car exhaust systems. The automotive industry accounts for approximately 80% of using Pt. The platinum emission rate has been estimated to be 0.5-0.8 μgPt/km from traffic. The second largest consumer is the chemical industry. Platinum is used as a catalyst in many reactions such as hydrogenation, dehydrogenation, and isomerization [43].

2.7 Gold

Au compound are commonly found in oxidation states +1 and +3 and maybe appear at oxidation states +1, +2, +3, +4, +5 and +7. Table 2.4 shows some physical and chemical properties [44].

Table 2.4 The physical and chemical properties of Gold.

Properties	Value
Atomic mass	196.97
Atomic number	79
Density	19.3 g/cm^3
Melting point	1,064 ^{o}C

Approximately 88% of all gold is used for fabrication and 12% for investment and bullion stocks. The gold for fabrication is used primarily in jewelry; this use accounts for approximately 85%. The balance is mostly used in electronics, dental appliances, medals, and commemorative objects of various types [44].

2.8 Yttria stabilized zircronia (YSZ)

Yttria stabilized zircronia (YSZ) is the fluorite-type electrolyte ceramic which consist of Zirconium dioxide (ZrO_2) stabilized by addition of yttrium oxide (Y_2O_3) (Figure 2.12). Oxygen–ion conductors are of the most common anionic conducting ceramics used in heterogeneous catalysis. The best known fluorite-type oxide–ion conductor is acceptor, ZrO_2. Pure zirconia has poor ionic conductivity. The accepter doping agent are introduced into the cation sublattice to stabilize the cubic structure at lower temperatures and to increase the concentration of oxygen vacancies which are required for ionic conduction via vacancy transport (oxygen migration) [45].

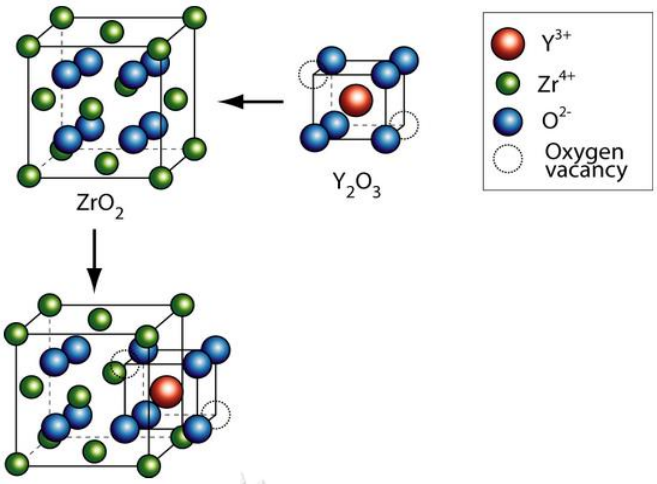

Figure 2.12 YSZ fluorite crystal cubic structure [46].

Stabilized ZrO_2 has been used almost exclusively as the electrolyte in solid oxide fuel cells (SOFCs) because the material possesses an adequate level of oxygen-ion conductivity and exhibits desirable stability in both oxidizing and reducing atmospheres. Among the various stabilized zirconias, the Y_20_3-stabilized material is the most common [47].

The exhibiting of high oxide–ion conductivity at temperatures above 700 °C, YSZ is the most common oxygen ion conductive electrolyte used for catalytic applications in solid electrolyte cell reactors and has been the mainstay commercially workable SOFCs. YSZ is a material with unique characteristics, with enhanced chemical stability as compared to other ceramic conductors, and this is suitable also for liquid phase applications. YSZ membranes can maintain a stable cubic fluorite structure between room temperature and 2700 °C. As a result, the use of YSZ is more promising for high temperature applications, such as membrane reactors and gas separation. The YSZ membranes also exhibit considerable high oxygen ionic conductivity and extremely low thermal conductivity at high temperatures [45].

CHAPTER III
METHODOLOGY

3.1 Pt-YSZ cell preparation

3.3.1 Wireless configuration

Au was sputtered on two equal opposite section on the same side of YSZ disk of 20 mm diameter and 1.2 mm thickness. In the middle of YSZ-cell was left 10 mm width for Pt deposition (Figure 3.1)

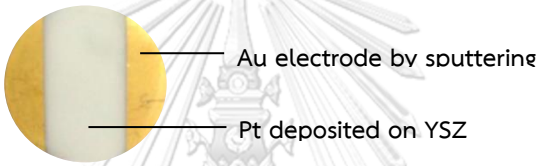

Figure 3.1 Pt-YSZ cell used in NEMCA experiments.

The sputtered samples were prepared using a magnetron sputtering system (JOEL: JFC-1100E Ion sputtering). High purity argon has been used as sputtering gas and the substrate temperature was kept stable during the deposition. The discharge characteristics have been controlled using a variable DC power supply. Pt has been used as sputtering target. A thin Pt film was sputter-deposited on the 10 mm width of YSZ dick varied Pt loading by increasing time [23], From the experiment, the four different Pt loading catalysts were compared to impregnation method that was deposited in range of 0.1-0.6 mgPt/m^2 by using sputtering time i.e. 10, 15, 20 and 25 sec at 10 mA and working pressure of 10 to 1 Pa.

The deposition of Pt on the 10 mm width of YSZ-cell was impregnated by dropping 250 µL H_2PtCl_6 aqueous solutions varied concentration for four different Pt loading. From the experiment, the catalysts were impregnated in range of 0.1-0.6

mgPt/m^2. And then it was dried overnight in flowing air. Finally, the YSZ disk was reduced by temperature at 250°C with pure H_2 (110 ml/min) gas for 2 hours [48].

3.1.2 Conventional configuration

Au was selected as counter electrode because of its negligible catalytic activity in propane oxidation [13]. Au was sputtered in the middle of YSZ-cell 10 mm width on the YSZ disk of 20 mm diameter and 1.2 mm thickness. And sputtered Pt film was deposited at the opposite point of Au on the other side of the YSZ disk. (Figure 3.1)

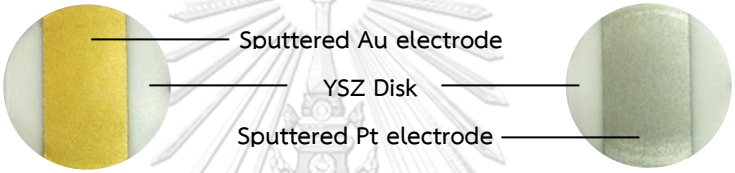

Figure 3.2 Pt-YSZ cell used in NEMCA experiments.

Sputtered samples were prepared by using a magnetron sputtering system. High purity argon has been used as sputtering gas and the substrate temperature was kept stable during the deposition. The discharge characteristics have been controlled using a variable DC power supply. Pt has been used as sputtering target. A thin Pt film was sputter-deposited on the 10 mm width of YSZ dick by JOEL: JFC-1100E Ion sputtering at 10 mA and working pressure of 10 to 1 Pa varied by increasing thickness of Pt film with increasing time [23]. In this research, Au and Pt electrodes spent the sputtering time for 45 minutes which was enough for using as film electrodes.

3.2 NEMCA experiment

The Pt and Au electrodes of YSZ disk were attached to each other that were connected to a power supply. In conventional configuration, the potential difference of -1 to +1 V could be imposed on the Pt and Au electrodes of a Pt-YSZ disk which was inside a quartz vessel in a furnace.

Propane oxidation was chosen as a model reaction that was carried out at 200-500°c. Reactants gases consisted of standard of 10% of oxygen in helium and 3% of propane in helium by varied the inlet partial pressure of oxygen P_{O2} from 1 to 5 kPa for conventional configuration, 5 kPa for wireless configuration and the inlet partial pressure of propane was kept constant P_{C3H8} = 1 kPa. Then this mixture was diluted by highly pure helium (99.99%) and was fed to the vessel under the total gas flow rate of 100 cm^3/min (STP).

At various temperatures and potential differences, the gas product was analyzed for CO_2 concentrations. It could be converted into reaction rates and Faradaic yield by using equation (5) and (6), respectively.

The rate enhancement ratio (**ρ**) is determined by $\rho = (r / r^0)$ (5)

The Faradaic efficiency (**Λ**) is determined by $\Lambda = (r - r^0) / (I / nF)$ (6)

Where r^0 is the catalytic rate at open circuit,

r is the electrochemically promoted catalytic rate,

I is the applied current,

n is the charge of the promotion ion, and

F is Faraday's constant (96485 $c.mol^{-1}$) [20]

The diagram of the experimental equipment is shown in Figure 3.3

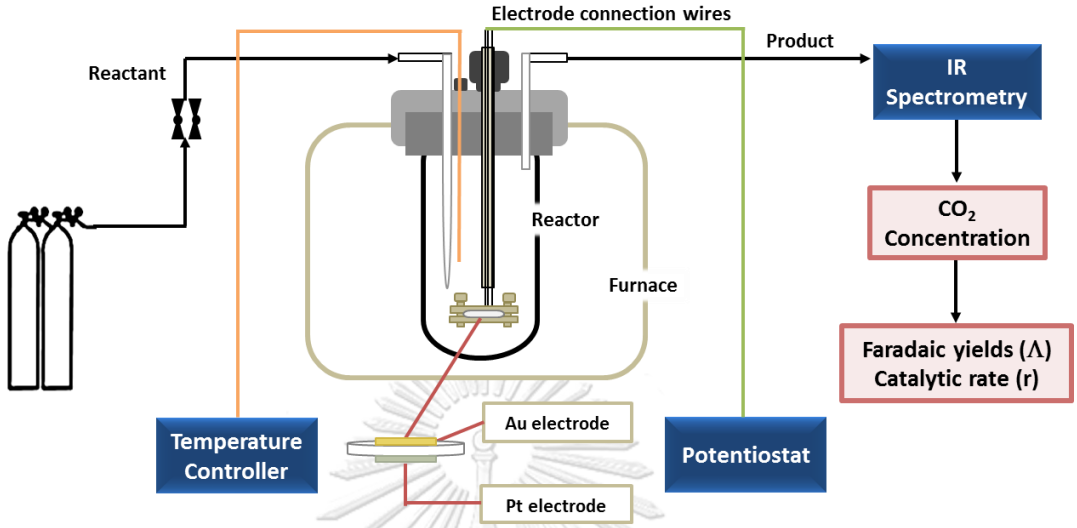

Figure 3.3 Schematic diagram of the experimental apparatuses adapted from C. Kokkofitis, (2005) [3]

3.3 Catalyst characterization

Inductively Coupled Plasma (ICP) spectroscopy technique was used to verify the concentrations of the Pt loading deposited by wet impregnation method and the sputtered-Pt loading. The Pt loading in sputtering method was determined by using a combination of solution of hydrochloric and nitric acid (Aqua Regia) in mole ratio of 1:3. The Pt film was removed from YSZ to aqua regia. The diluted solutions of different Pt loading were analyzed and plotted the calibration curve for calculate Pt loading of the different Pt sputtering time on YSZ disks. The Pt loading in wet impregnation method was determined by the diluted preparation solution after depositing on YSZ.

The morphology and external surface structure of the deposited Pt on YSZ disk were determined by Scanning Electron Microscopy (SEM) technique. The JEOL JSM-35 CF scanning electron microscope was operated at 15 kV. SEM micrographs of the different Pt loading of top view surface in wireless configuration for both of two preparation methods, external catalyst surface, and cross section of Pt on YSZ were determined before and after being used as catalyst on propane oxidation reaction in conventional configuration

The crystalline phase of the fresh and used sputtered Pt catalyst electrodes and YSZ were examined by X-ray diffraction (X-ray diffraction performed in the SIXMENS D5000) connected x-ray diffractometer connected to computer with Diffract ZT version 3.3 program with Cu-Kαl radiation, λ = 1.54 Å. In conventional configuration, the fresh and after Pt-YSZ was used as catalyst on propane oxidation reaction, XRD patterns were recorded in the 2θ range between 20° and 90°, with scan step size of 0.021 and step time of 88.5 s per step.

CHAPTER IV
RESULTS AND DISCUSSION

4.1 Wireless configuration Pt-YSZ

4.1.1 Catalyst characterization

The Pt loading by impregnation and sputtering coat method on YSZ disk was determined by Inductively Coupled Plasma (ICP) technique.

Table 4.1 Pt loading deposited by impregnation and sputtering methods was determined from ICP technique.

Method	Wet impregnation		Sputtering coat	
Pt loading ($mgPt/m^2$)	WI 1	0.1146	SP 1	0.1105
	WI 2	0.2925	SP 2	0.2680
	WI 3	0.4586	SP 3	0.4254
	WI 4	0.6615	SP 4	0.5829

Table 4.1 shows the result of different Pt loading by wet impregnation preparation. The catalysts prepared by two different preparation techniques were compared. The result shows that the values of deposited Pt of catalysts WI1 to WI4 were 0.11, 0.29, 0.46, and 0.66 $mgPt/m^2$ respectively. Pt loading by sputtering method had a result in the different Pt loading. To elaborate, the Pt loading of catalysts SP1 to SP4 were 0.11, 0.27, 0.43, and 0.58 $mgPt/m^2$ respectively. Pt loadings from two different preparation techniques were not different. The largest difference of Pt loading between two preparation methods was found in WI4 and SP4 around 11%.

Figure 4.1.1 and 4..1.2 show the surface morphology of the impregnation and sputtered Pt working electrodes at 0.11 mgPt/m^2 on YSZ disk after being used as catalyst of propane oxidation reaction was examined by Scanning Electron Microscopy (SEM) technique. Moreover, the elemental distribution was determined by Energy dispersion X-ray Spectroscopy. The JEOL JSM-35 CF scanning electron microscope was operated at 15 kV.

(a) (b)

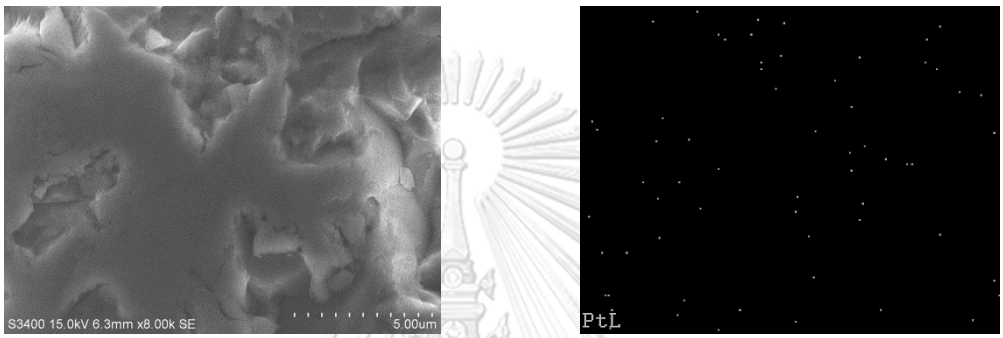

Figure 4.1.1 (a) SEM and (b) EDX micrographs of catalyst-electrode Pt-YSZ by wet impregnation method

(a) (b)

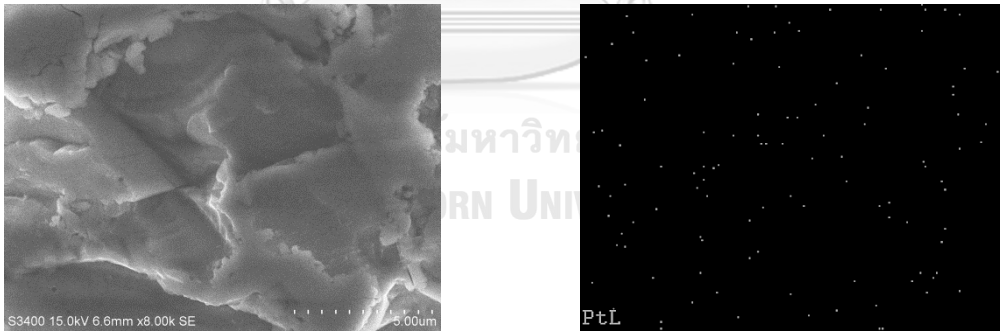

Figure 4.1.2 (a) SEM and (b) EDX micrographs of catalyst-electrode Pt-YSZ by sputtering method

4.1.2 Catalytic activity at open-circuit voltage and Electrochemically promoted catalytic activity under closed-circuit

Figure 4.1.3 and 4.1.4 show the effects of the electrical potential difference between the working and counter electrodes on the Faradaic efficiency (**Λ**). The inlet partial pressure of propane was kept constant at P_{C3H8} = 1 kPa and the inlet partial pressure of oxygen P_{O2} was varied from 5 kPa while the temperature was varied from 200 to 500 °C by different wireless configuration preparation method i.e. wet impregnation and sputtering coat.

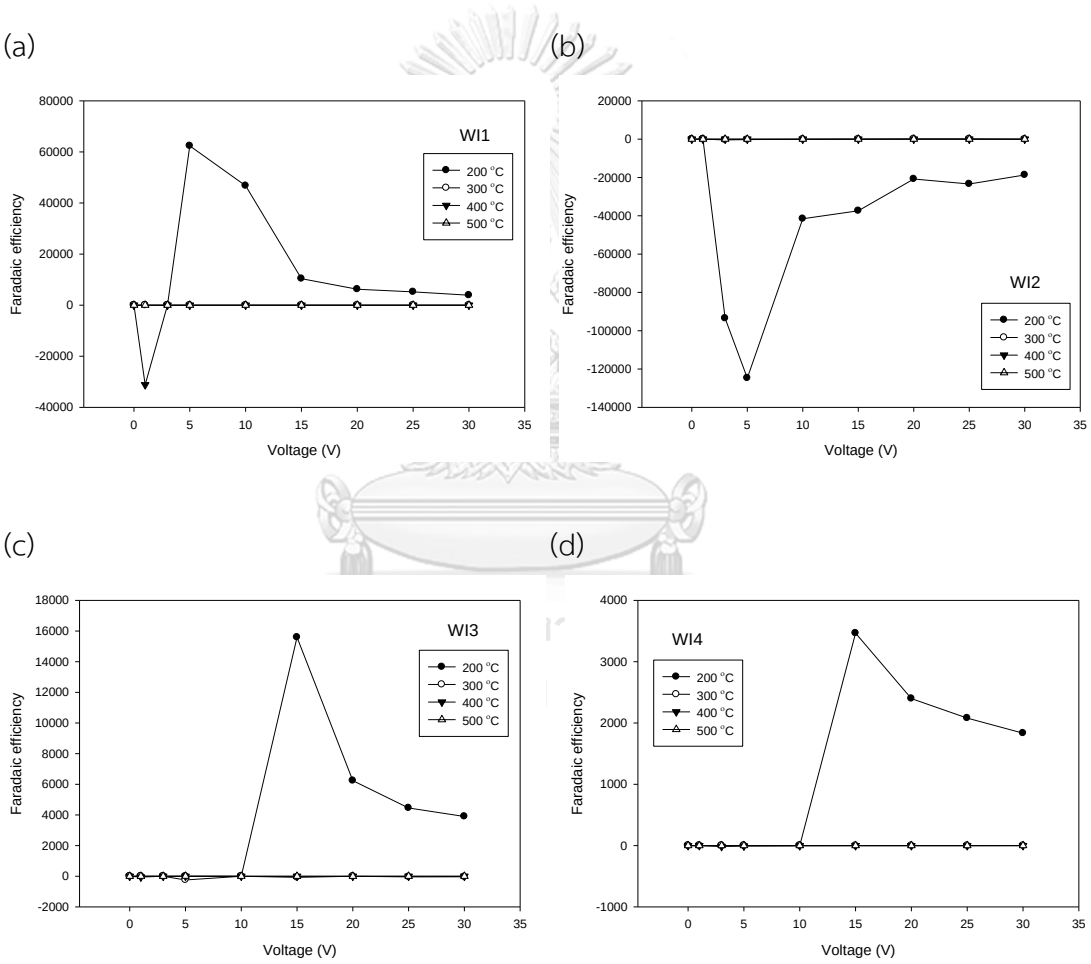

Figure 4.1.3 Dependence of Faradaic efficiency on the applied potential (V) at partial pressure of propane P_{C3H8} 1 kPa and oxygen P_{O2} 5 kPa and temperature 200 to 500 °C by wet impregnation method (a) WI1 = 0.11 mgPt/m^2, (b) WI2 = 0.29 mgPt/m^2, (c) WI3 = 0.46 mgPt/m^2 and (d) WI4 = 0.66 mgPt/m^2.

Figure 4.1.3 shows the faradaic efficiency of electrochemically promoting the catalytic activity with Pt-YSZ prepared by wet impregnation method. In figure 4.3 (a), (c) and (d), the largest Faradaic efficiency was 6.2×10^{4} at 5 V for WI1, 1.4×10^{4} at 15 V for WI3, and 3.4×10^{3} at 15 V for WI4 at temperature 200 °C. According to figure 4.3 (b), at 200 °C, the values of Faradaic efficiency became negative from 5 to 30 V. It can be seen that at 300 to 500 °C, figure 4.3 (a) - (d) did not show NEMCA effect. To sum up, in terms of wet impregnation method, these results did not obviously show a trend of the faradaic efficiency values.

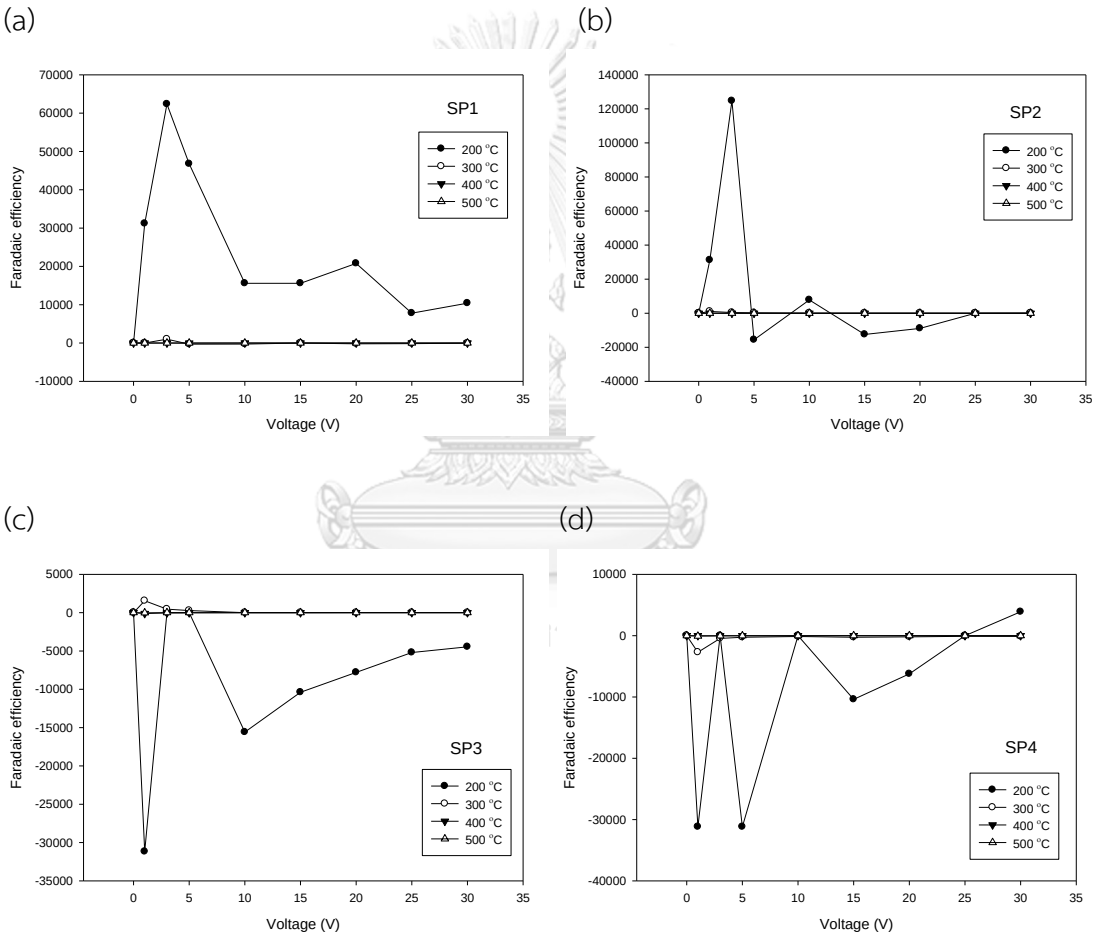

Figure 4.1.4 Dependence of Faradaic efficiency on the applied potential (V) at partial pressure of propane P_{C3H8} 1 kPa and oxygen P_{O2} 5 kPa and temperature 200 to 500 °C by sputtering method (a) SP1 = 0.11 mgPt/m^2, (b) SP2 = 0.27 mgPt/m^2, (c) SP3 = 0.43 mgPt/m^2 and (d) SP4 = 0.58 mgPt/m^2.

Figure 4.1.4 shows the faradaic efficiency of electrochemically promoting the catalytic activity with Pt-YSZ prepared by sputtering method. The lowest Pt loading shows NEMCA effect on the largest potential range because the deposited Pt from sputtering was formed as particles which could disperse well on YSZ surface. At higher Pt loading, Pt particles may be formed as the larger particles. As the result, the gradient of potential did not occur and also NEMCA effect did not show. In figure 4.1.4 (a), the largest Faradaic efficiency was 6.2×10^{4} at 5 V, 200 ℃ for SP1. From Figure 4.1.4 (b), at 200 ℃, 3 V, the highest Faradaic efficiency of 1.2×10^{5} was observed. It became negative value at 5 V. The negative values of Faradaic efficiency were observed at 200 ℃ from 1 to 30 V for SP3 (figure 4.1.4 (c)) and from 1 to 20 for SP4 (figure 4.1.4 (d)). And NEMCA effect did not show at temperature of 300 to 500 ℃ in figure 4.1.4 (a) - (d). Figure 4.1.5 shows SEM and EDX micrographs of catalyst-electrode Pt-YSZ in wireless configuration system of both preparation methods, i.e. (a) SP1 (b) SP4 (c) WI1 and (d) WI4.

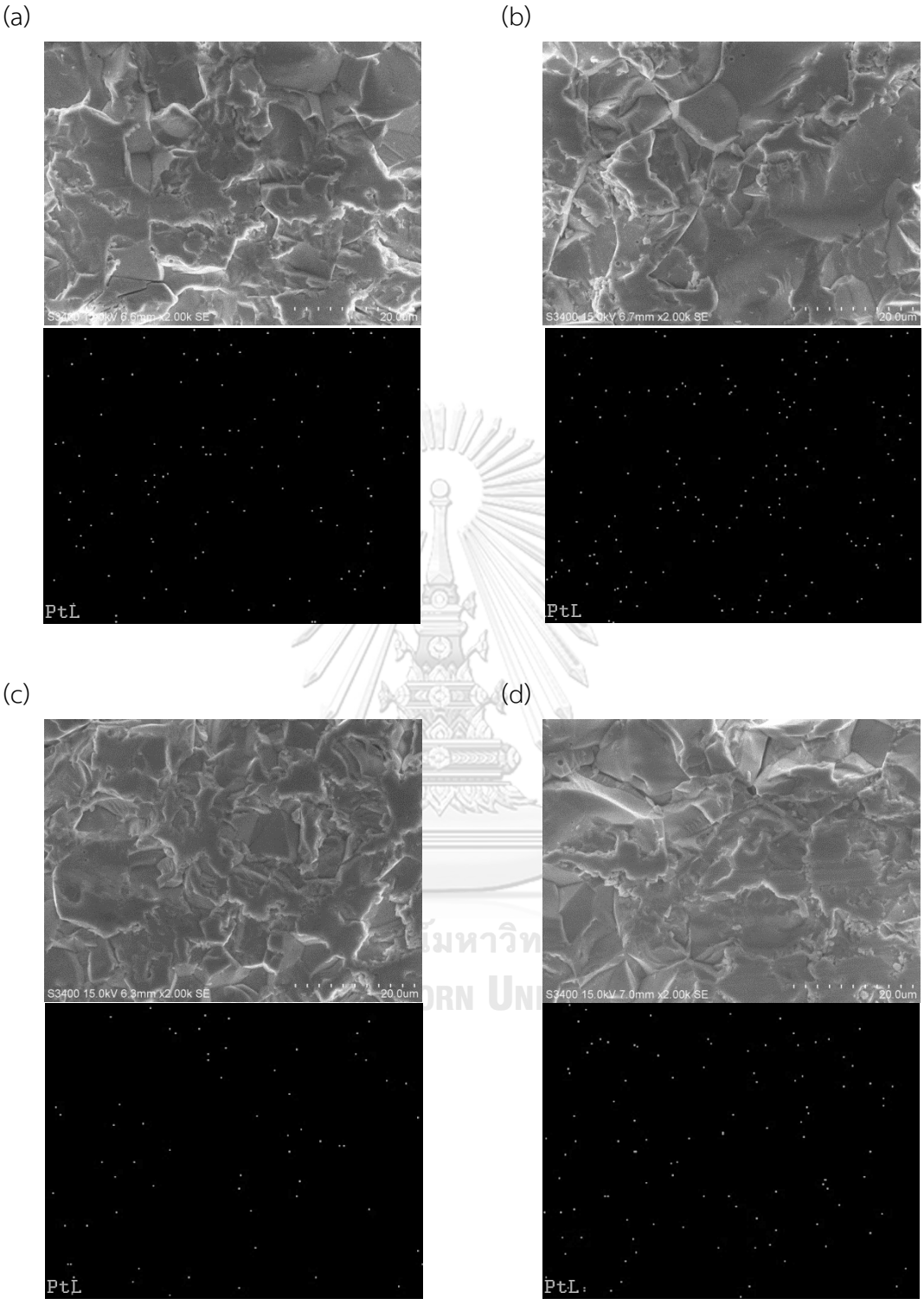

Figure 4.1.5 SEM and EDX micrographs of catalyst-electrode Pt-YSZ in wireless configuration of (a) SP1 (b) SP4 (c) WI1 and (d) WI4

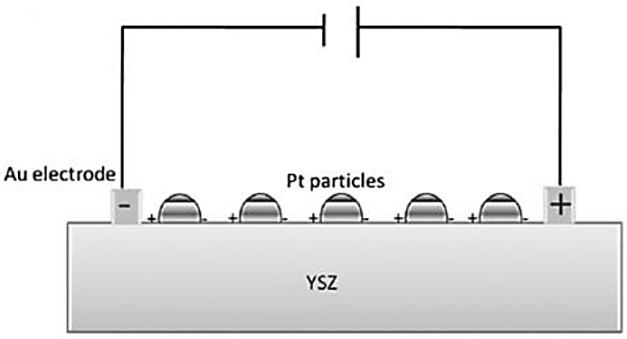

Figure 4.1.6 Cross section of the wireless configuration [45].

In this system, a Pt was deposited between two gold electrodes on a YSZ disk (figure 4.1.6). This configuration, the catalytic is not directly polarized. Part of the catalytic material is polarized with a positive charge, while the other part of Pt used as a working electrode is polarized with a negative charge. In this way, one part of the catalyst acts as an anode and the other as a cathode. There is no uniform catalyst work function as in the case. The catalytic activity is the result of the negative and positive polarization of the catalytic material [45].

At high temperatures, the balance between adsorption and desorption rates of oxygen ions at Pt surface probably showed that oxygen ions desorption was higher than oxygen ions adsorption. The larger negative polarization area of Pt particles with decreased coverage of oxygen ions and effective double-layer caused the weak NEMCA effects. [20, 45].

(a)

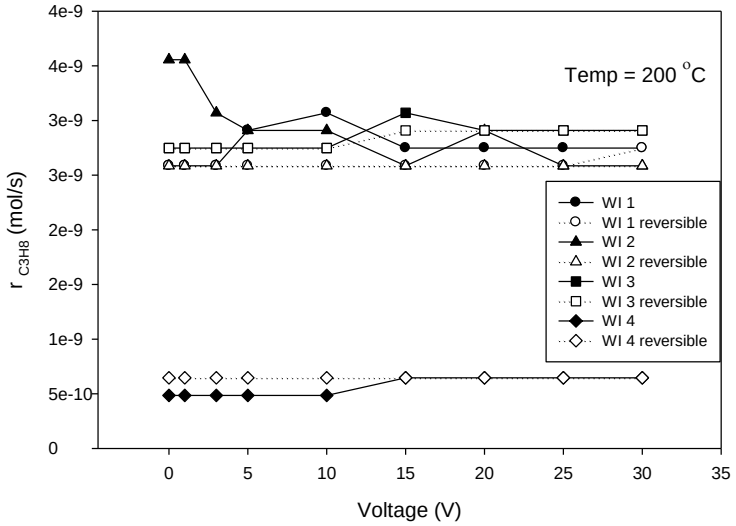

(b)

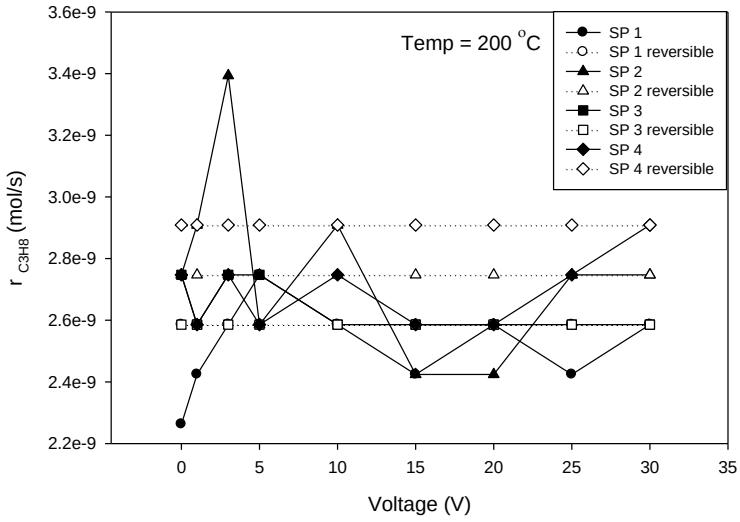

Figure 4.1.7 Dependence of catalytic rate on the applied potential (V) at partial pressure of propane P_{C3H8} 1 kPa and oxygen P_{O2} 5 kPa and temperature 200°C by (a) wet impregnation method and (b) sputtering method.

Figure 4.1.7 shows that at temperature of 200°C and different Pt loading by wet impregnation and sputtering methods, rate values of increasing potential (closed symbols) were not equal to rate values of decreasing potential (open symbols). It meant that the catalytic reaction of wireless system was irreversible reaction while NEMCA effect was the phenomena that occurred via a potential supply. There is no

uniform catalyst work function where platinum is used as the working electrode. The resulting effect is a combination between the activity of negatively and positively and of current on catalyst potential. [39]

The wireless configuration of catalytic electrode of Pt-YSZ used less Pt loading than the conventional configuration. The NEMCA performances of wireless configuration were observed at 200 °C. These results were irreversible reaction by using either impregnation or sputtering methods that did not indicated NEMCA effect. Furthermore, this configuration also used more applied potential because of different coverage of oxygen ions on Pt-YSZ. Therefore, the conventional configuration was studied in part 4.2.

4.2 Conventional configuration Pt-YSZ

4.2.1 Catalyst characterization

The Pt loading sputtered on YSZ disk was determined by Inductively Coupled Plasma (ICP) technique. The Pt loading that was sputtered with sputtering time about 45 min was 84.82 mgPt/ m^2

The surface morphology of the sputtered Pt working electrode on YSZ disk before and after used as catalyst of propane oxidation reaction was determined by Scanning Electron Microscopy (SEM) technique. The JEOL JSM-35 CF scanning electron microscope was operated at 15 kV.

(a) (b)

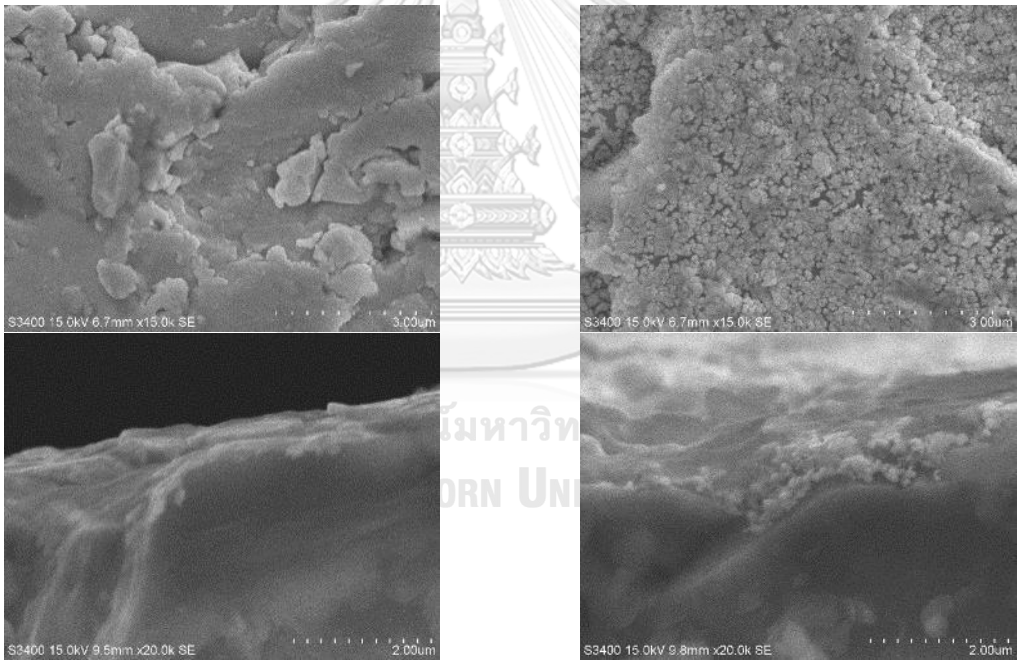

Figure 4.2.1 SEM micrographs of fresh and used catalyst-electrode Pt-YSZ that (a) before and (b) after used as catalyst of propane oxidation

Figure 4.2.1 presents the surface morphology of metal catalyst electrode of Pt deposited on YSZ before and after exposure to reactive the gas mixture by Scanning Electron Microscopy (SEM) technique. The fresh Pt-YSZ showed a smooth

and thin metallic film on the YSZ support. In addition, after the propane oxidation reaction, Pt catalyst film exhibited rougher surface morphology. This indicated that oxide formation under O^{2-} was supplied to surface.

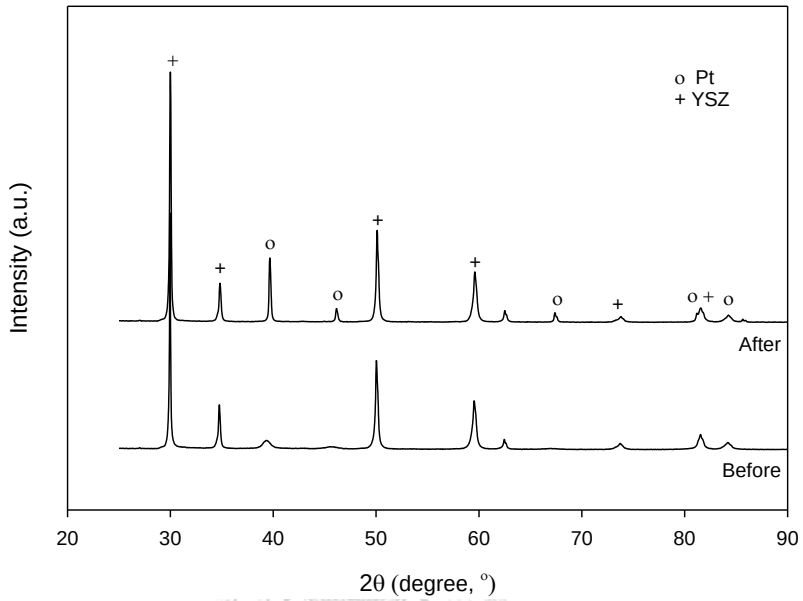

Figure 4.2.2 XRD pattern of the Pt-YSZ catalyst

The XRD patterns of the fresh and used sputtered Pt-YSZ are shown in figure 4.2.2. The characteristic diffraction peak of Pt and YSZ were detected by XRD [15]. Fresh sputtered catalyst showed broad peak reflections of the metal Pt form at 39.3°. After exposure to propane reaction, the sharp peak of metal Pt appeared at 39.7°, 46.1° and 67.3°.

4.2.2 Catalytic activity at open-circuit voltage and Electrochemically promoted catalytic activity under closed-circuit

The catalytic reaction rate was studied at 200-500 °C and at 1 kPa partial pressure of propane. The partial pressure of inlet oxygen ranged from 1.0 to 5.0 kPa. Helium was used as the diluent gas, and the total volumetric flow rate was 100 cm^3/min. At all temperatures, the only reaction product which was detected was CO_2. After that, the rate of CO_2 was calculated to be the rate of propane. Therefore, in all of the results, reaction rate was presented in mole of propane per second.

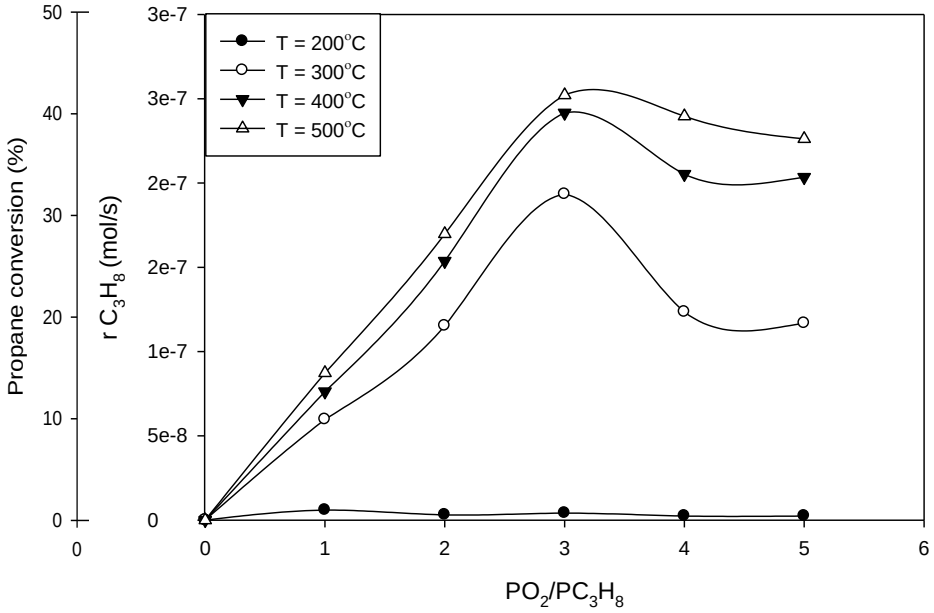

Figure 4.2.3 Dependence of the reaction rate and propane conversion on P_{O2}/P_{C3H8} at various reaction temperatures, partial pressure of propane P_{C3H8} 1 kPa.

Figure 4.2.3 shows the dependence of reaction rate on oxygen partial pressure. The partial pressure of propane was kept at 1 kPa, and the temperature was varied from 200 to 500 °C. It was found that the catalytic reaction rate under open-circuit increased with increasing temperatures. Figure 4.2.3 shows that at temperature range of 300 to 500 °C, at low oxygen partial pressure, the reaction rate increased with increasing oxygen partial pressure until a maximum value reached at 3

kPa, then decreased with higher oxygen partial pressure. These results conform to Langmuir-Hinshelwood model that at low partial pressure of oxygen, the surface of catalyst is mostly covered by propane which is the reactant gas so the reaction rate is low. When the oxygen partial pressure increases, the covered oxygen gas on catalyst surface slightly increases so the catalytic rate reaches to maximum value. On the other hand, at high partial pressure of oxygen, the surface coverage of propane is extremely decreased therefore the catalytic rate becomes low [49]. The study of C. Kokkofitis revealed that, at low oxygen partial pressure, the catalyst was reduced, and high reaction rates were observed. As oxygen partial pressure increased, the Pt surface was oxidized, and its catalytic activity dropped. Thus, after reaching a maximum value, the rate decreased with P_{O2} [2, 3].

(a)

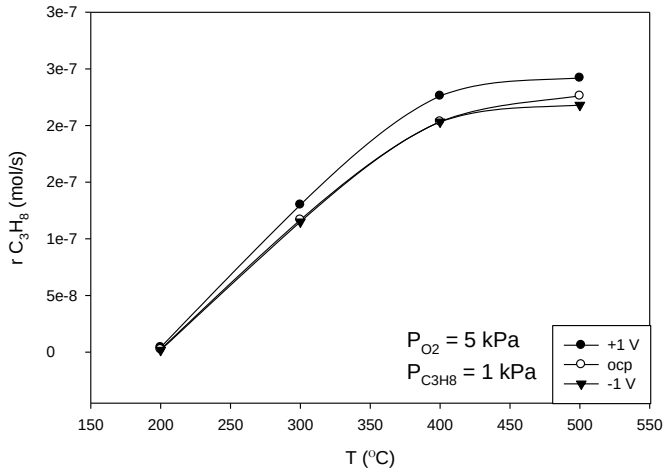

(b)

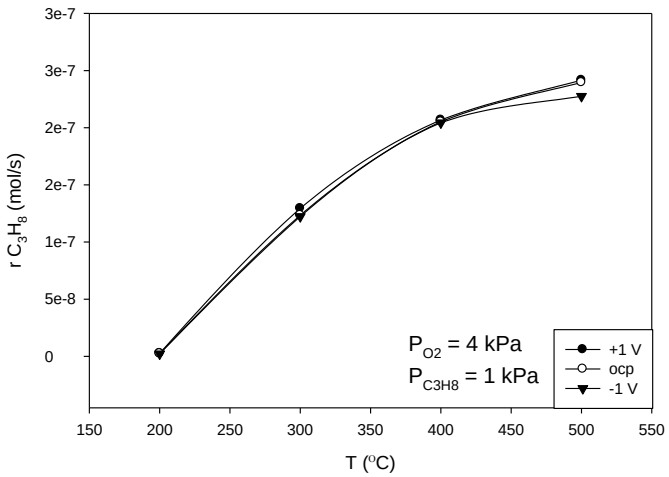

(c)

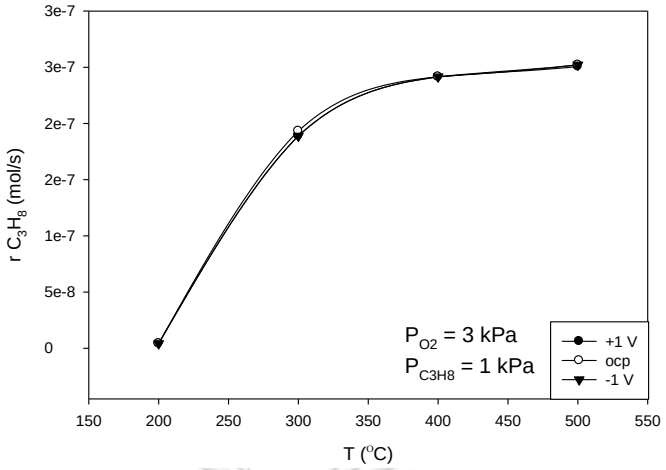

(d)

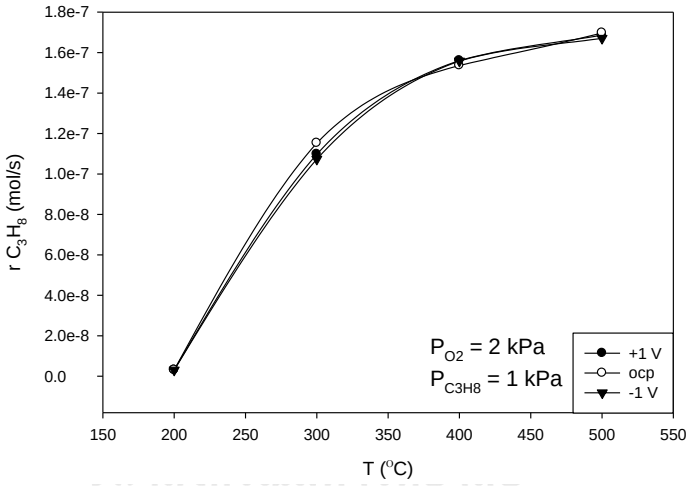

(e)

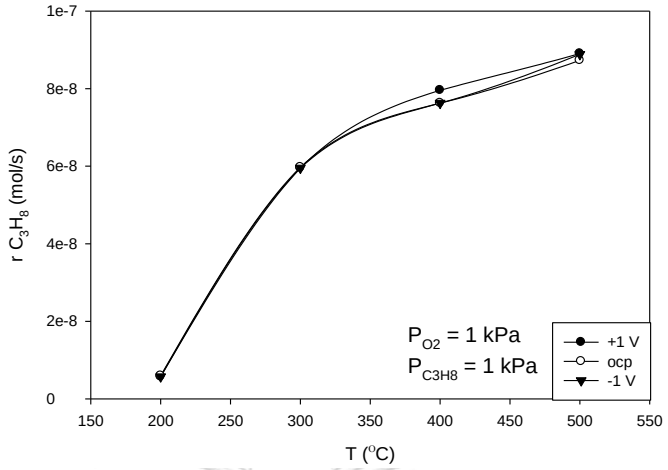

Figure 4.2.4 Effect of temperature on the catalytic rate under open-circuit and positive and negative (±1 V) potential at constant P_{C3H8} = 1 kPa and (a) P_{O2} = 5 kPa (b) P_{O2} = 4 kPa (c) P_{O2} = 3 kPa (d) P_{O2} = 2kPa and (e) P_{O2} = 1 kPa.

Figure 4.2.4 shows the effect of temperature on the catalytic rate under open-circuit, and positive (+1 V) and negative (-1 V) potential conditions at P_{C3H8} = 1 kPa and different oxygen partial pressures from 1 to 5 kPa. As shown in the figure, under (a) P_{O2} = 5 kPa and (b) P_{O2} = 4 kPa, the reaction rates increased with increasing temperature and increasing potential at above a temperature of 200 °C which behave a purely electrophobic type [19, 36].

As shown in the figure, under (c) P_{O2} = 3 kPa, (d) P_{O2} = 2 kPa and (e) P_{O2} = 1 kPa, the reaction rates of reactant clearly increased at temperature of 200 to 350 °C because the reaction rates were fast, the reaction was controlled by the transfer of the reactant to the surface. And the reaction rates slightly increased at 400 to 500 °C because at high temperature region corresponded to bulk mass transfer between the gas phase and Pt surface area. Mass transfer controlled reactions can be obtained through the using of higher operating temperatures [1].

(a)

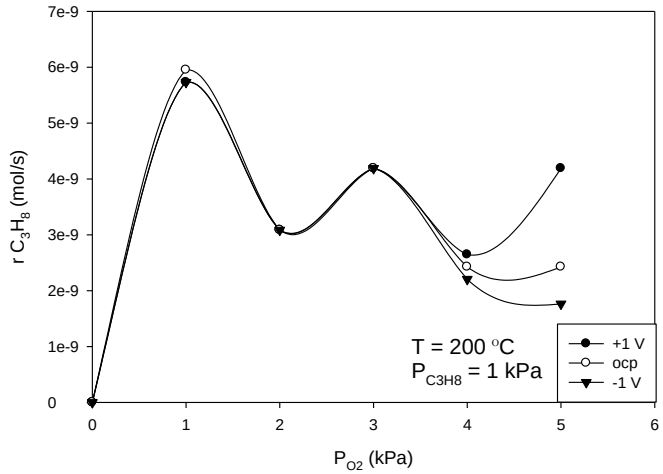
7e-9
6e-9
5e-9
4e-9
3e-9
2e-9
1e-9
0
r C3H8 (mol/s)
0
1
2
3
4
5
6
PO2 (kPa)
T = 200 °C
PC3H8 = 1 kPa
+1 V
ocp
-1 V

(b)

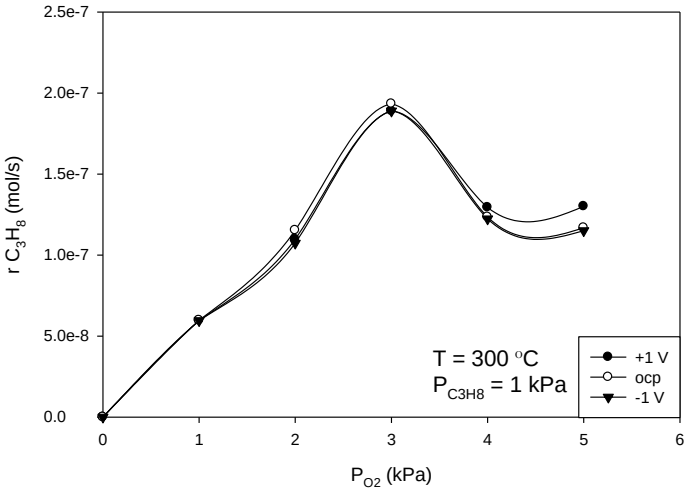
2.5e-7
2.0e-7
1.5e-7
1.0e-7
5.0e-8
0.0
r C3H8 (mol/s)
0
1
2
3
4
5
6
PO2 (kPa)
T = 300 °C
PC3H8 = 1 kPa
+1 V
ocp
-1 V

(c)

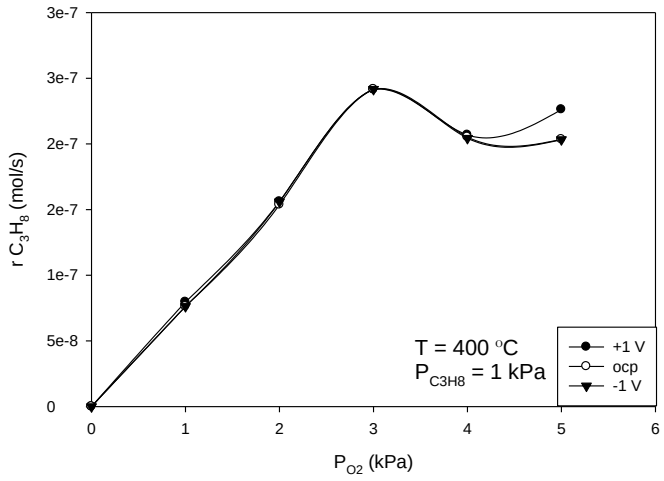

(d)

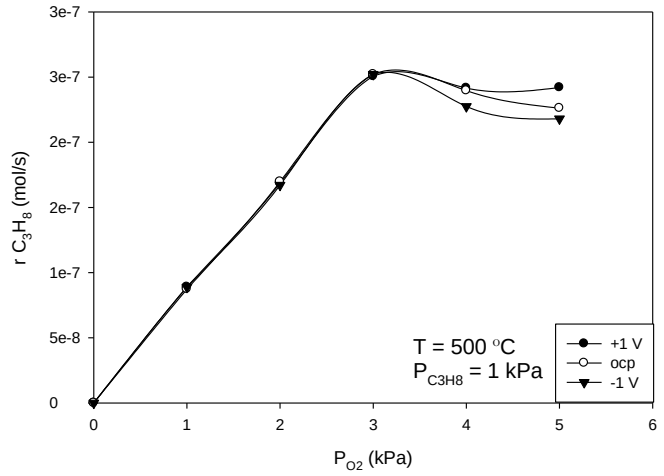

Figure 4.2.5 Effect of P_{O2} on the CO_2 formation catalytic rate under open-circuit and positive and negative (±1 V) potential at constant P_{C3H8} = 1 kPa and T = (a) 200°C (b) 300°C (c) 400°C and (d) 500°C.

Figure 4.2.5 shows the effect of oxygen partial pressure on the CO_2 formation catalytic rate under open circuit and positive and negative potential polarization at constant propane partial pressure P_{C3H8} = 1 kPa. As shown in the figure, the electrophobic type behavior was observed under high oxygen partial pressure (>3

kPa) at different temperatures of 200, 300, 400 and 500°C [19, 36]. This behavior was electrophobic type that was in agreement with figure 4.2.4 (a) P_{O2} = 5 kPa and (b) P_{O2} = 4 kPa.

(a)

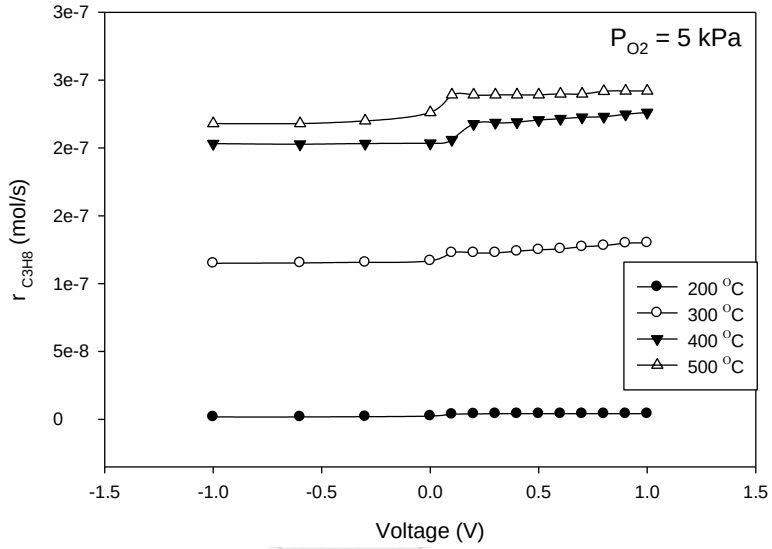

(b)

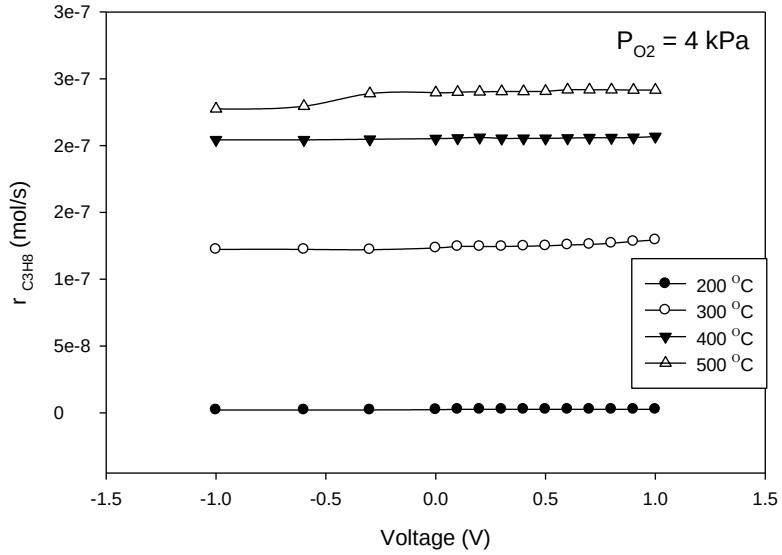

(c)

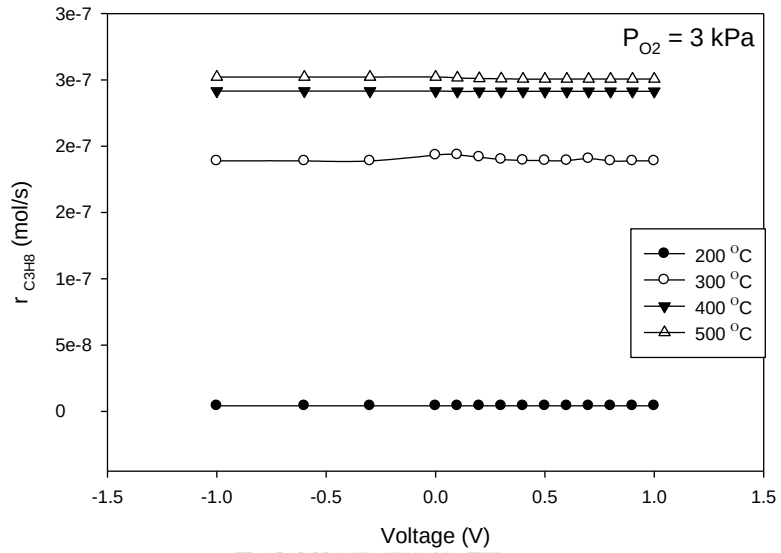
P$_{O2}$ = 3 kPa
r $_{C3H8}$ (mol/s)
3e-7
3e-7
2e-7
2e-7
1e-7
5e-8
0
-1.5
-1.0
-0.5
0.0
0.5
1.0
1.5
Voltage (V)
200 °C
300 °C
400 °C
500 °C

(d)

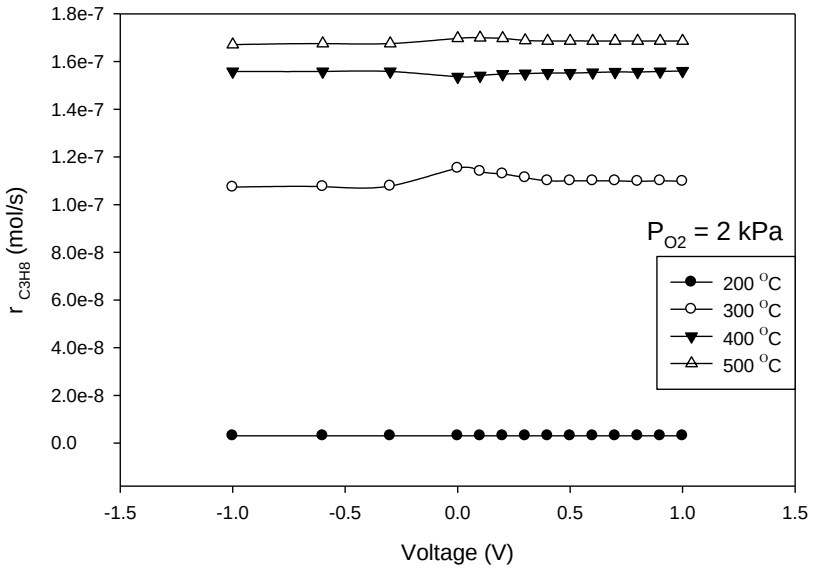
P$_{O2}$ = 2 kPa
r $_{C3H8}$ (mol/s)
1.8e-7
1.6e-7
1.4e-7
1.2e-7
1.0e-7
8.0e-8
6.0e-8
4.0e-8
2.0e-8
0.0
-1.5
-1.0
-0.5
0.0
0.5
1.0
1.5
Voltage (V)
200 °C
300 °C
400 °C
500 °C

(e)

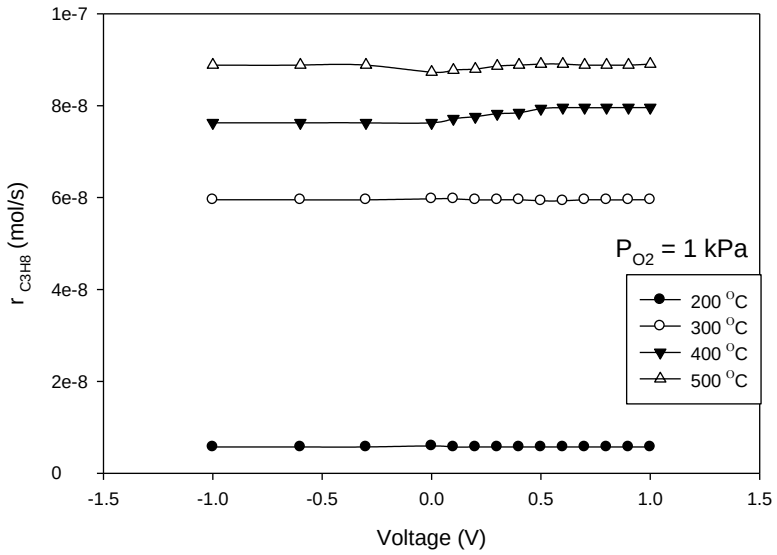

Figure 4.2.6 Dependence of rate of reaction on the applied potential (V) at temperature range 200-500 °C and at partial pressure of propane P_{C3H8} 1 kPa and oxygen P_{O2} (a) 1 kPa, (b) 2 kPa, (c) 3 kPa, (d) 4 kPa and (e) 5 kPa

Figure 4.2.6 shows electrochemical promotion results of propane oxidation on a Pt-sputtered film. Figure 4.2.6 (a) and (b), the rate of propane increases in positive polarization current and decreases in negative polarization current. At partial pressure of oxygen (c) P_{O2} = 3 kPa at 200°C to 500°C, (d) P_{O2} = 2 kPa at 300°C and 500°C, and (e) P_{O2} = 1 kPa at 200°C and 300°C shows that the reaction rate, r, decreased at positive potential and at 500°C it increased at both of positive and negative potential.

From figure 4.2.3, open-circuit condition at low P_{O2}/P_{C3H8}, the surface of catalyst reduced, and the reaction rates increased. At higher P_{O2}/P_{C3H8}, the reaction rates decreased because the surface of catalyst was oxidized [3]. In figure 4.2.6 (a) and (b), at P_{O2} 5 and 4 kPa, clearly indicates the effects of electrochemical promotion that the potential induces the increase of catalytic activity. The applied current, the reaction rate increased because the O^{2-} was pumped to the surface of

platinum and then reacted with oxygen reactant to product formation [19, 20]. At low P_{O2} condition, figure 4.2.6 (c) and (d) at P_{O2} 3 and 2 kPa at, reaction rate decreased with applied positive potential that agree with the result presented in the left side of figure 4.2.3. These behavior was electrophilic type of NEMCA [19, 20], where a critical P_{O2}/P_{C3H8} at 3 kPa was observed where electrochemical promotion of catalysis behavior changed, between electrophobic and electrophilic type behavior.

(a)

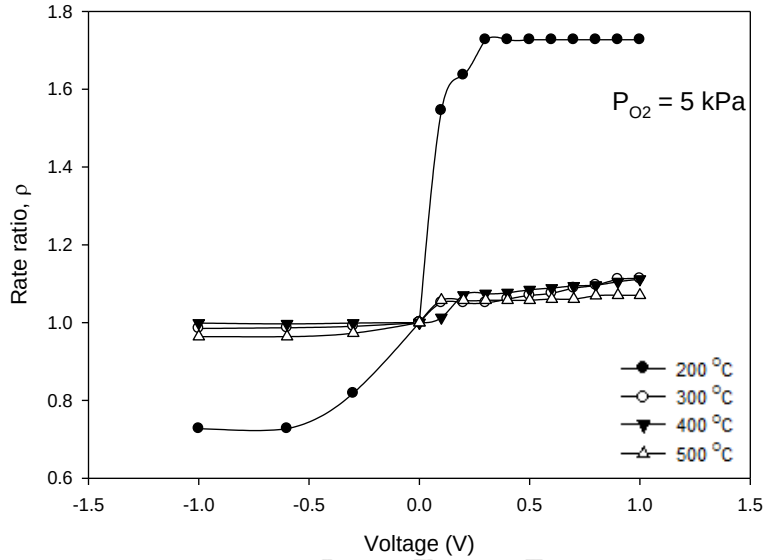

(b)

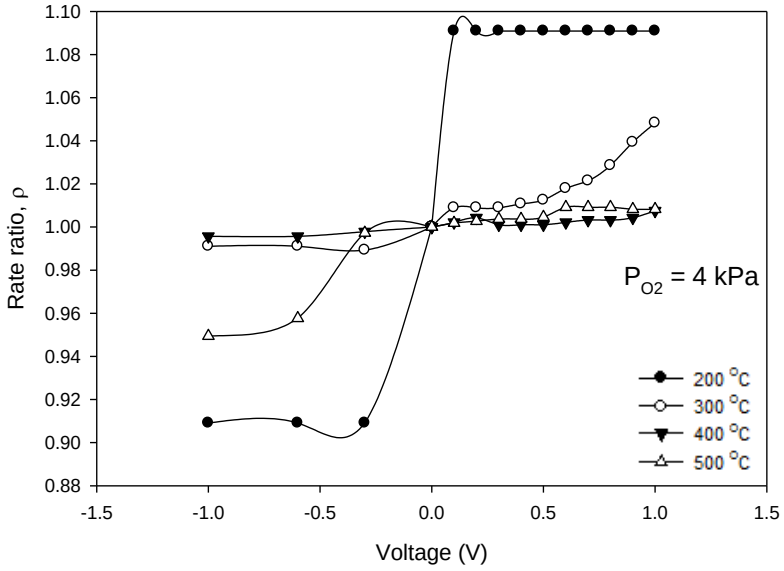

(c)

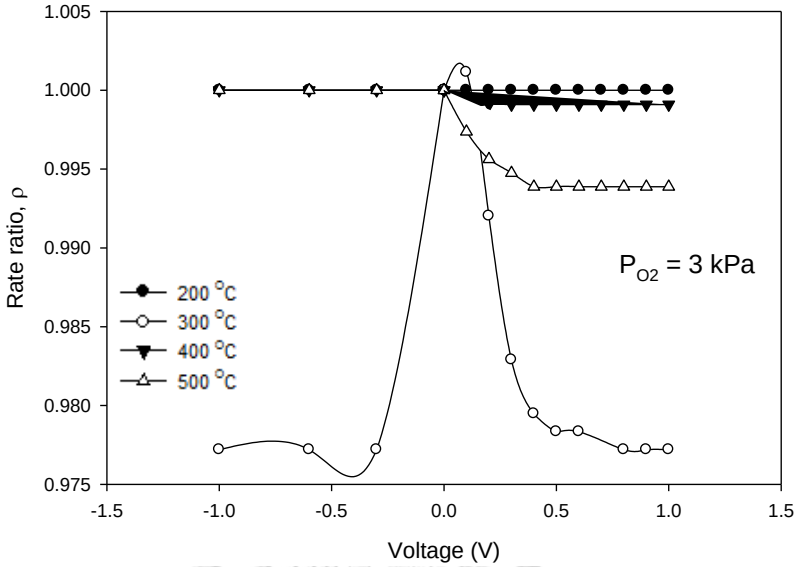
1.005
1.000
0.995
0.990
0.985
0.980
0.975
Rate ratio, ρ
-1.5
-1.0
-0.5
0.0
0.5
1.0
1.5
Voltage (V)
200 °C
300 °C
400 °C
500 °C
P$_{O2}$ = 3 kPa

(d)

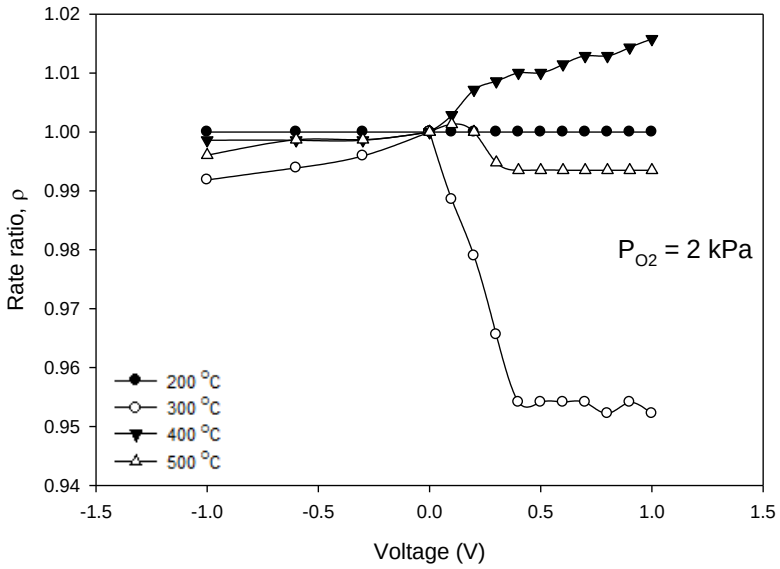
1.02
1.01
1.00
0.99
0.98
0.97
0.96
0.95
0.94
Rate ratio, ρ
-1.5
-1.0
-0.5
0.0
0.5
1.0
1.5
Voltage (V)
200 °C
300 °C
400 °C
500 °C
P$_{O2}$ = 2 kPa

(e)

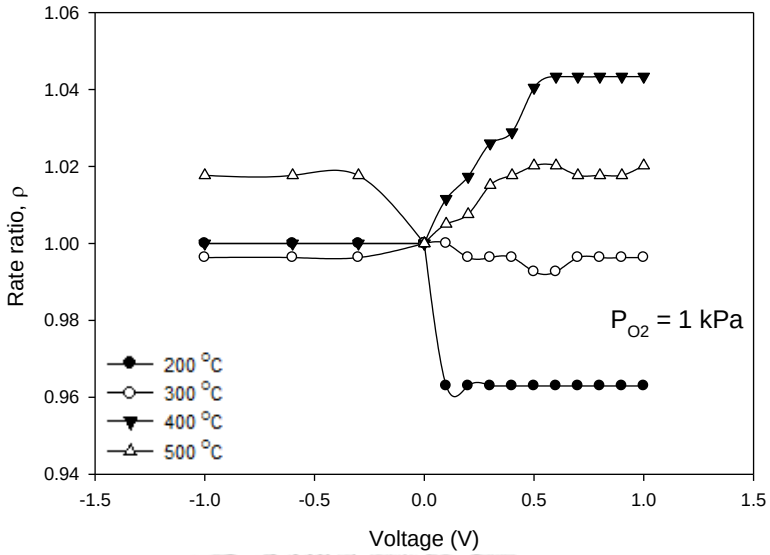

Figure 4.2.7 Dependence of rate enhancement ratio, ρ, on the applied potential (V) at partial pressure of propane P_{C3H8} = 1 kPa and oxygen (a) P_{O2} = 5 kPa, (b) P_{O2} = 4 kPa, (c) P_{O2} = 3 kPa, (d) P_{O2} = 2 kPa and (e) P_{O2} = 1 kPa.

Figure 4.2.7 shows the variation of rate enhancement ratio, ρ, with the applied potential at the propane partial pressure 1 kPa at four different temperatures 200, 300, 400 and 500°C for conventional sputtering Pt catalyst electrode. Figure 4.2.7 at partial pressure of oxygen (a) P_{O2} = 5 kPa and (b) P_{O2} = 4 kPa shows that the reaction ratio, ρ, increased at positive potential and decreased at negative potential. From figure 4.2.3, under open-circuit, reaction rate increased at high oxygen partial pressure i.e. P_{O2} = 4 and 5 kPa. Under closed circuit, when oxygen ions, O^{2-}, were pumped, oxygen surface adsorption decreased, so the reaction rate increased. Exhibits of figure 4.2.7 (a) P_{O2} = 5 kPa and (b) P_{O2} = 4 kPa were electrophobic behavior type. The observed exhibit was in agreement with the rules of promotion set by Vayenas and co-workers [19, 20]. Rate enhancement ratio, ρ, reached to 1.7 at partial pressure of oxygen P_{O2} = 5 kPa and at temperature of 200 °C.

Figure 4.2.7 at partial pressure of oxygen (c) P_{O2} = 3 kPa at 200°C to 500°C, (d) P_{O2} = 2 kPa at 300°C and 500°C, and (e) P_{O2} = 1 kPa at 200°C and 300°C shows that

the reaction ratio, ρ, decreased at positive potential. From figure 4.2.3, under open-circuit, reaction rate increased at oxygen partial pressure P_{O2} = 3, 2 and 1 kPa. Under closed circuit, when oxygen ions, O^{2-}, were pumped oxygen surface adsorption decreased so the reaction rate decrease. The observed exhibits were electrophilic behavior type. The only one condition of reaction ratio, ρ, at oxygen partial pressure P_{O2} = 1 kPa at 500°C was inverted volcano type that was in agreement with Kokkofitis and co-workers (2005, 2007) [3 ,26]. The results at temperature of 200°C to 400°C were electrophilic which were different with the study of Kokkofitis due to the different catalyst preparation, using Pt paste film in the previous study and sputtering method in this research.

Figure 4.2.8 to 4.2.12 show the effect of the electrical potential difference between the working and counter electrodes on the Faradaic efficiency (Λ). The inlet partial pressure of propane was kept constant at P_{C3H8} = 1 kPa and the inlet partial pressure of oxygen P_{O2} was varied from 1 to 5 kPa while the temperature was varied from 200 to 500 °C.

(a)

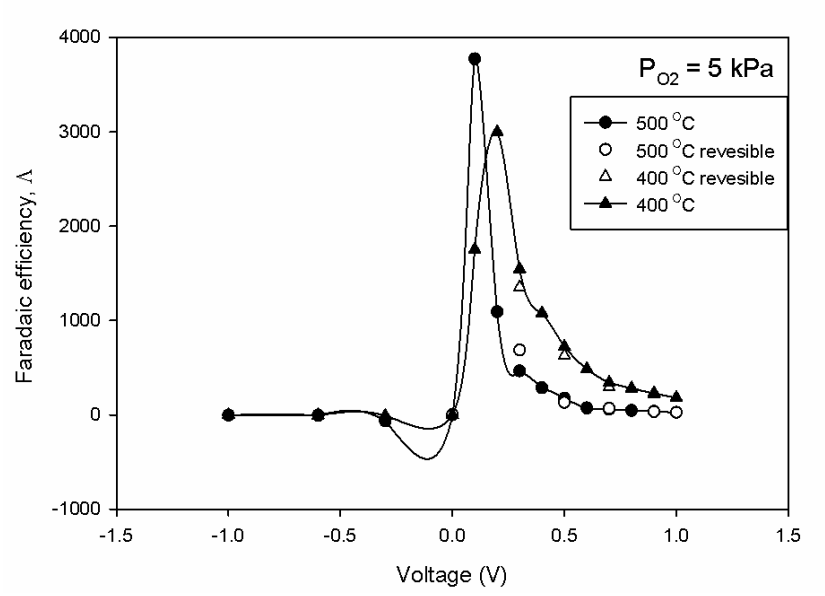

(b)

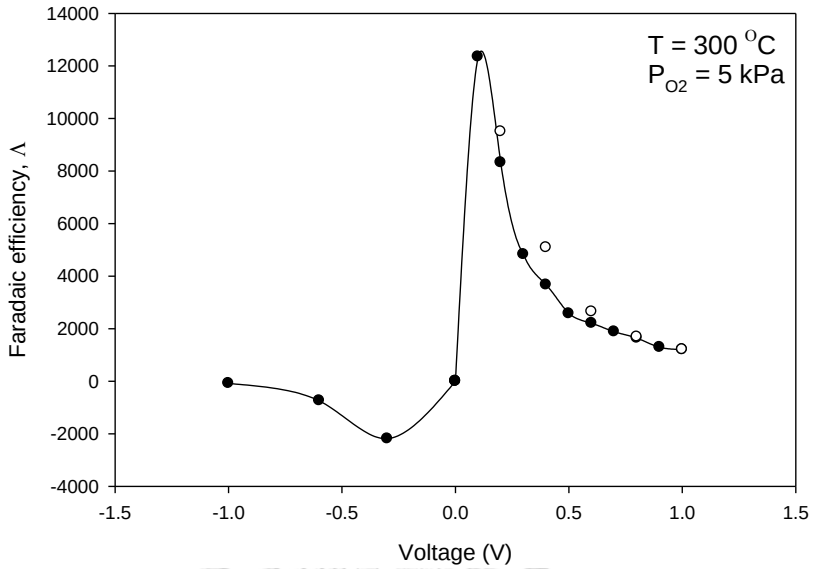

(c)

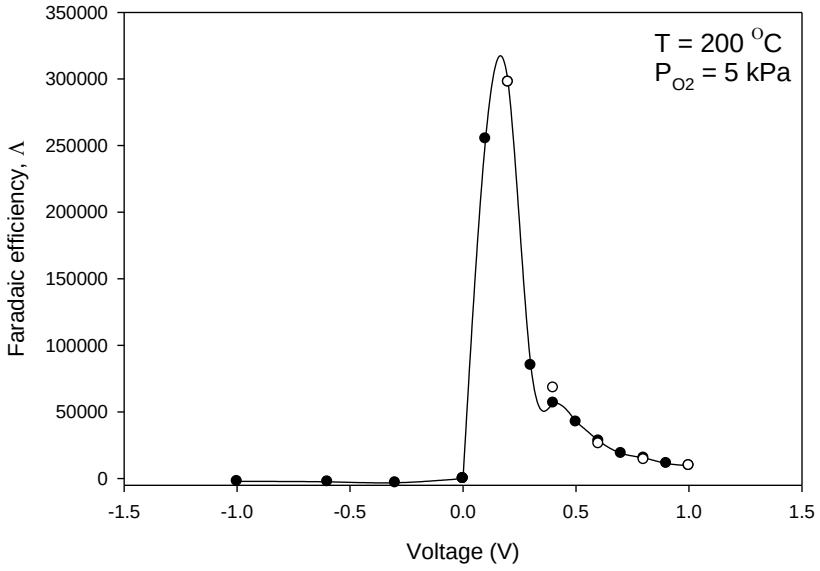

Figure 4.2.8 Dependence of Faradaic efficiency on the applied potential (V) at partial pressure of propane P_{C3H8} 1 kPa and oxygen P_{O2} 5 kPa and temperature (a) 500 °C and 400 °C, (b) 300 °C and (c) 200 °C (reversible value, ○)

(a)

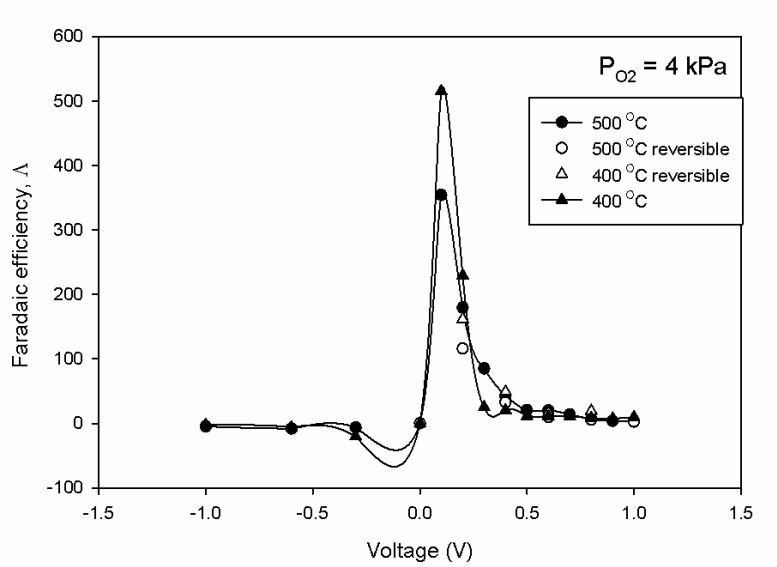
P_{O2} = 4 kPa
500 °C
500 °C reversible
400 °C reversible
400 °C
Faradaic efficiency, Λ
Voltage (V)
600
500
400
300
200
100
0
-100
-1.5
-1.0
-0.5
0.0
0.5
1.0
1.5

(b)

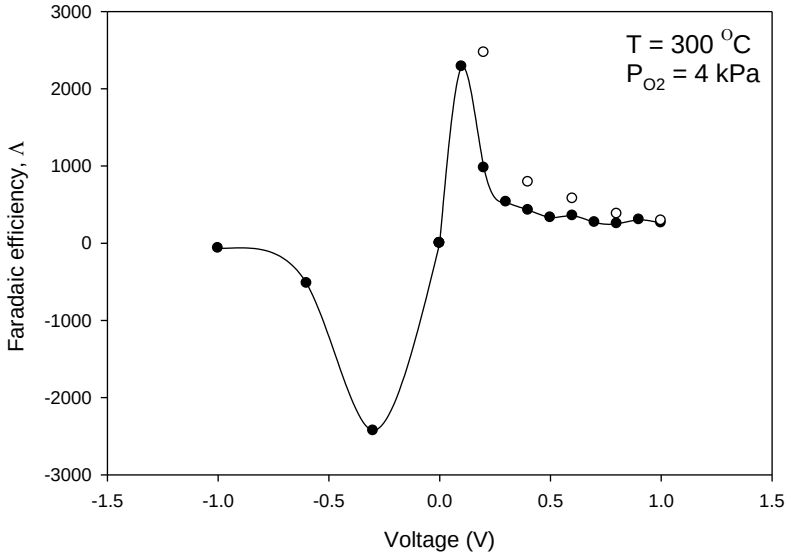
T = 300 °C
P_{O2} = 4 kPa
Faradaic efficiency, Λ
Voltage (V)
3000
2000
1000
0
-1000
-2000
-3000
-1.5
-1.0
-0.5
0.0
0.5
1.0
1.5

(c)

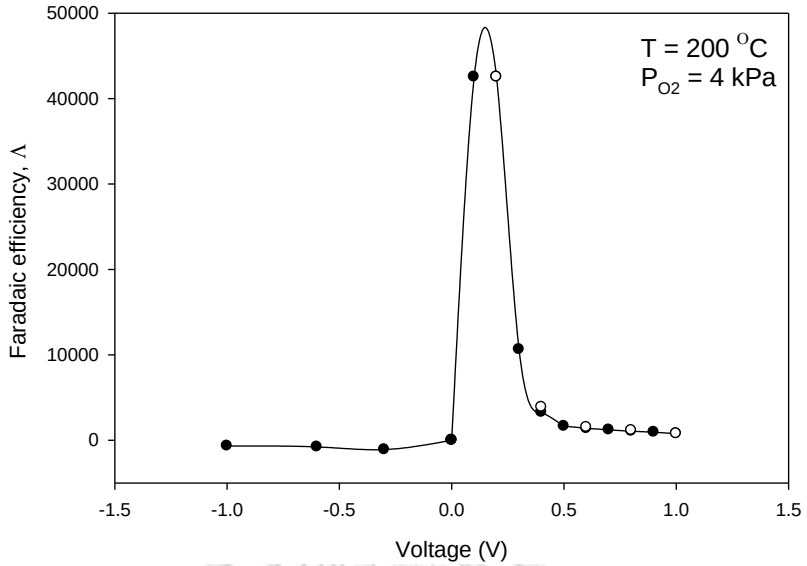

Figure 4.2.9 Dependence of Faradaic efficiency on the applied potential (V) at partial pressure of propane P_{C3H8} 1 kPa and oxygen P_{O2} 4 kPa and temperature of (a) 500 °C and 400 °C (b) 300 °C and (c) 200 °C (reversible value, ○)

Figure 4.2.8 and 4.2.9 show the dependence of faradaic efficiency on the electrical potential at the partial pressures of oxygen of 5 and 4 kPa respectively. In these two figures, high **Λ** values were observed at positive potential (O^{2-} pumped towards the catalyst). It can be seen that these behaviors were electrophobic type of NEMCA [19, 20]. The effect at positive potentials was more significant by up to a faradaic efficiency of 250,000 and 40,000 at P_{O2} of 5 and 4 kPa respectively at 200 °C.

The reversible faradaic efficiency behavior (open symbol, ○) was observed when an applied positive potential was decreased from 1 to 0 volt. It can be seen that faradaic efficiency was similar to faradaic efficiency with increasing positive potential from 0 to 1.

(a)

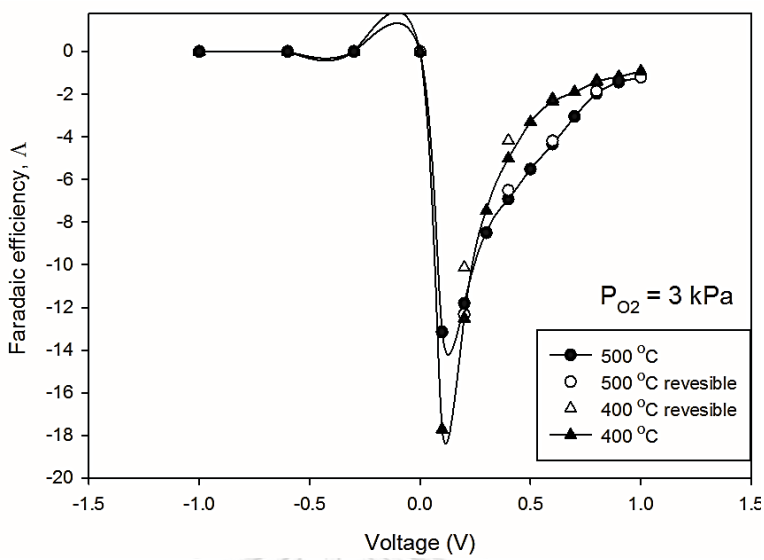
Faradaic efficiency, Λ
Voltage (V)
P_{O2} = 3 kPa
500 °C
500 °C revesible
400 °C revesible
400 °C

(b)

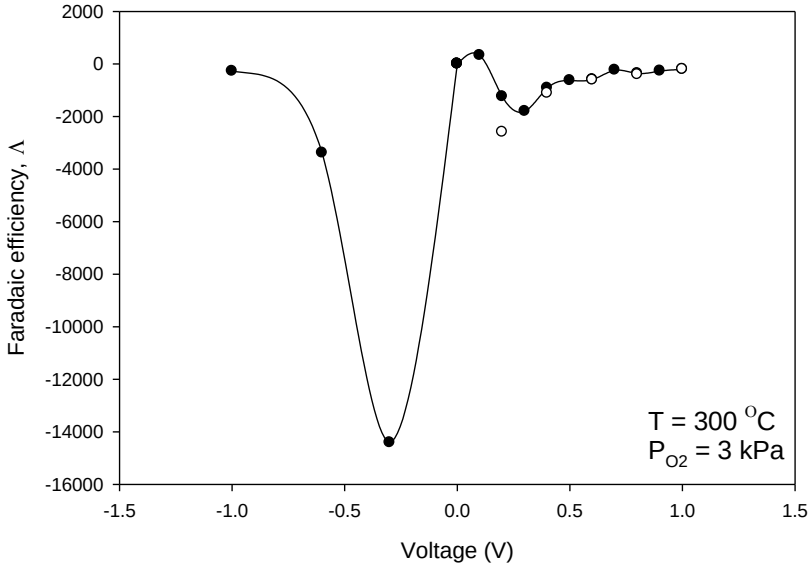
Faradaic efficiency, Λ
Voltage (V)
T = 300 °C
P_{O2} = 3 kPa

(c)

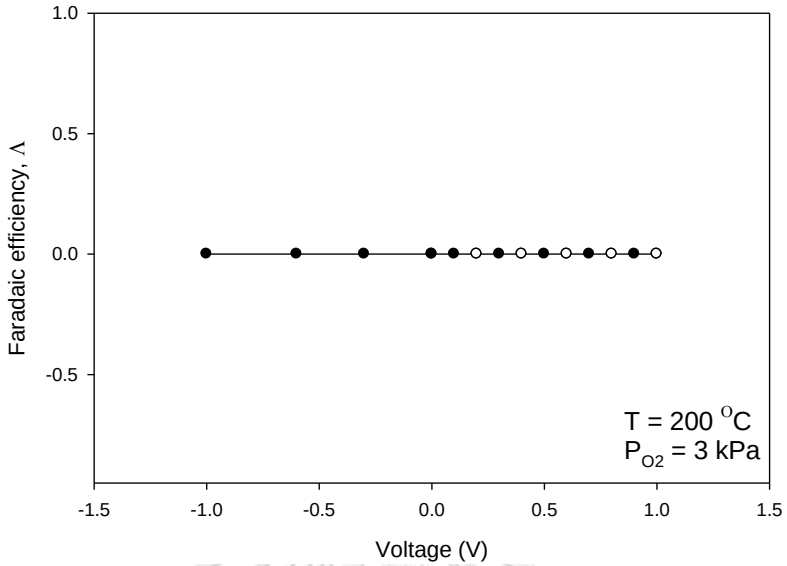

Figure 4.2.10 Dependence of Faradaic efficiency on the applied potential (V) at partial pressure of propane P_{C3H8} 1 kPa and oxygen P_{O2} 3 kPa and temperature of (a) 500 °C and 400 °C (b) 300 °C and (c) 200 °C (reversible value, ○)

(a)

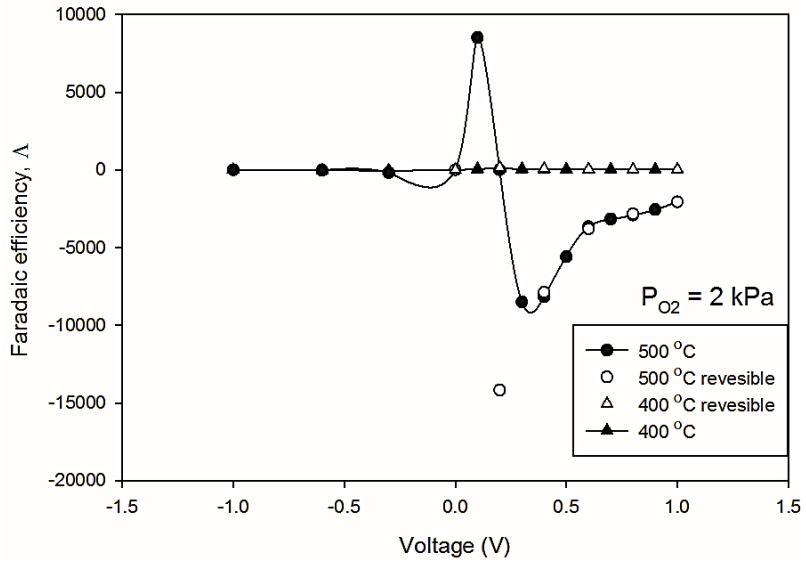

(b)

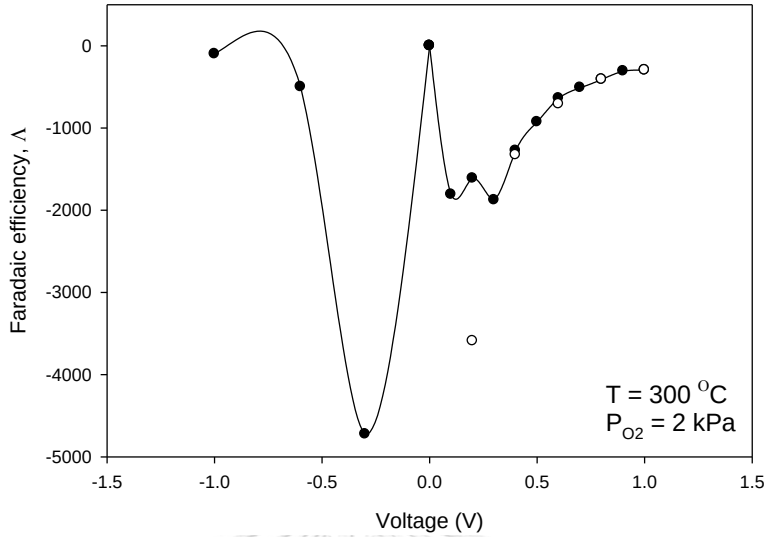

(c)

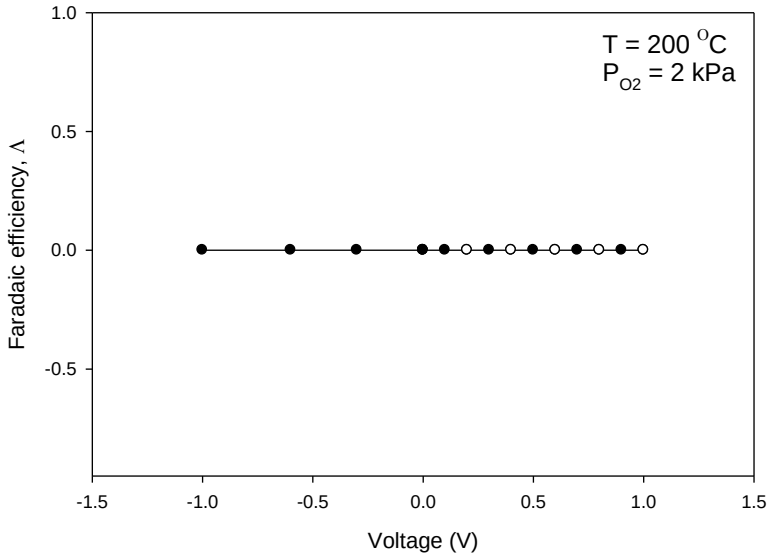

Figure 4.2.11 Dependence of Faradaic efficiency on the applied potential (V) at partial pressure of propane P_{C3H8} 1 kPa and oxygen P_{O2} 2 kPa and temperature of (a) 500 ℃ and 400 ℃ (b) 300 ℃ and (c) 200 ℃ (reversible value, ○)

Figure 4.2.10 and 4.2.11 show the dependence of faradaic efficiency on the electrical potential at the partial pressures of oxygen of 3 and 2 kPa. Faradaic

efficiency at temperatures of 300, 400 and 500 °C at positive potential condition shows electrophilic NEMCA behavior.

(a)

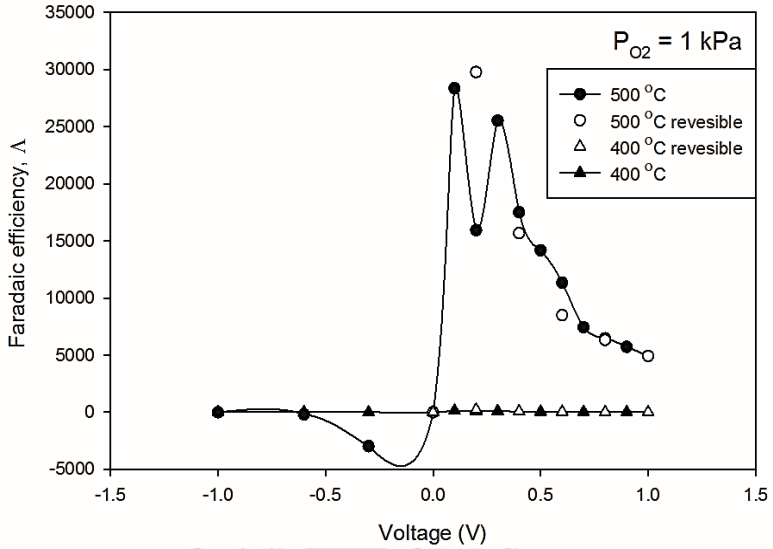

(b)

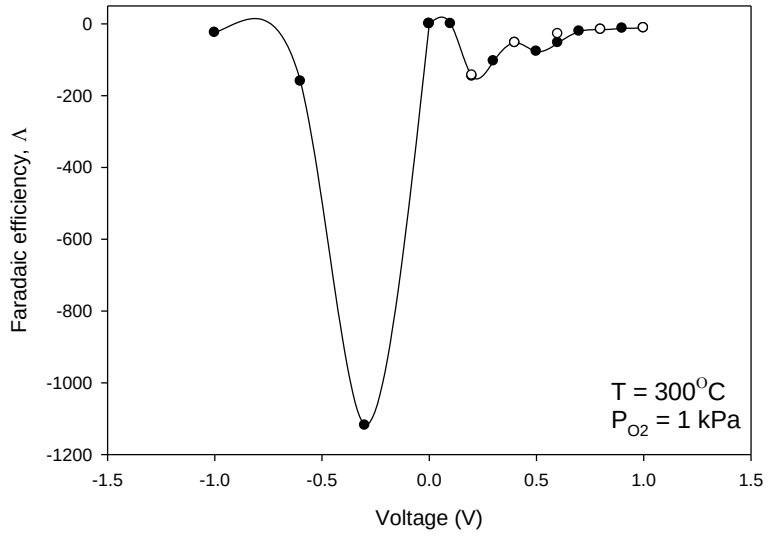

(c)

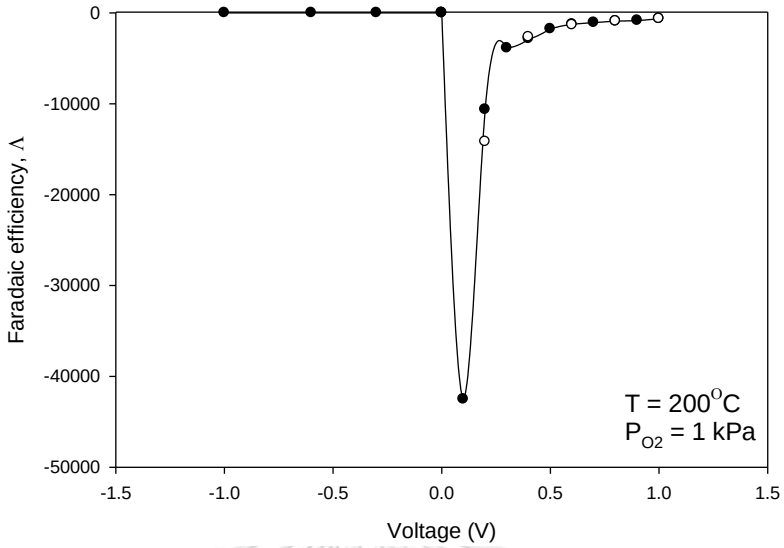

Figure 4.2.12 Dependence of Faradaic efficiency on voltage (V) at partial pressure of propane P_{C3H8} 1 kPa and oxygen P_{O2} (a.) 3 kPa, (b.) 2 kPa and (c.) 1 kPa.

(a)

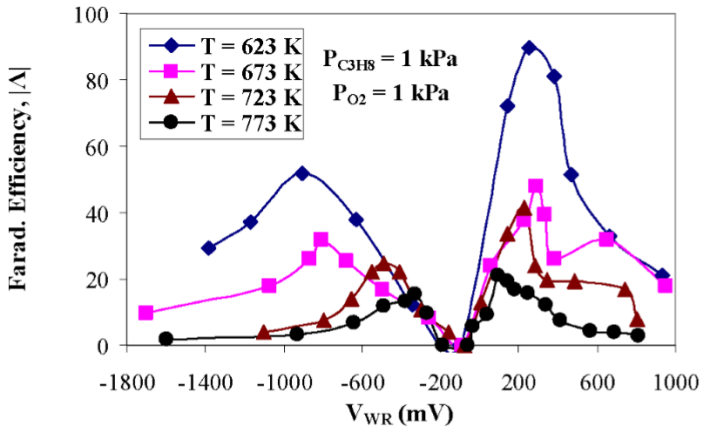

(b)

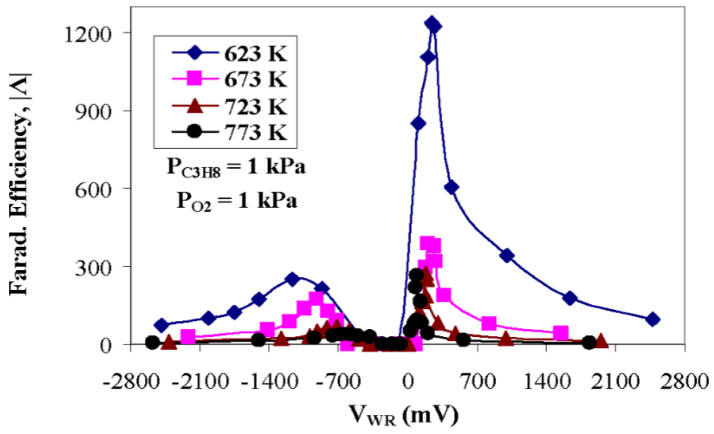

Figure 4.2.13 Effect of catalyst potential on the absolute Faradaic efficiency. P_{C3H8} = 1 kPa, P_{O2} = 1 kPa and temperature range 250 to 400°C for reactors (a) R2 and (b) R3. [3]

In figure 4.2.12, The Faradaic efficiency value partial pressure of oxygen 1 kPa could confusedly induce NEMCA effects at high temperature (500 °C). The present results disagree with Kotsionopoulos's study [27]. The study indicated that, in the range of temperature from 425 to 520°C and for P_{O2}/P_{C3H8} ratios which was lower than the stoichiometric ratio, the rate of propane combustion increased with applied currents and the promotion behavior were inverted volcano type of NEMCA [27].

Under closed circuit of Kokkofitis's study [3] in figure 4.2.13, when positive and negative current were applied, the reaction rate and Faradaic efficiency increased. The observed exhibits were inverted volcano type. The Faradaic efficiency, **Λ**, at oxygen partial pressure P_{O2} = 1 kPa was in disagreement with Kokkofitis and co-workers (2005, 2007) [3 ,26].

Figure 4.2.8 to 4.2.12, the reversible behavior of faradaic efficiency was observed when an applied positive potential was decreased from 1 to 0 volt. It can be seen that faradaic efficiency (open symbol, ○) was similar to faradaic efficiency with increasing positive potential from 0 to 1. The reversible reaction which depended on applied current confirmed NEMCA effects.

(a)

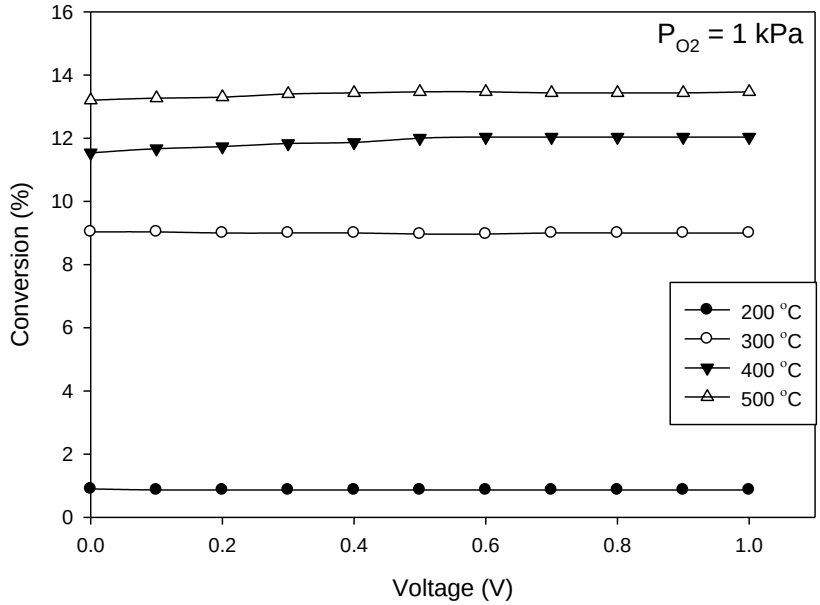
P$_{O2}$ = 1 kPa
Conversion (%)
Voltage (V)
200 °C
300 °C
400 °C
500 °C

(b)

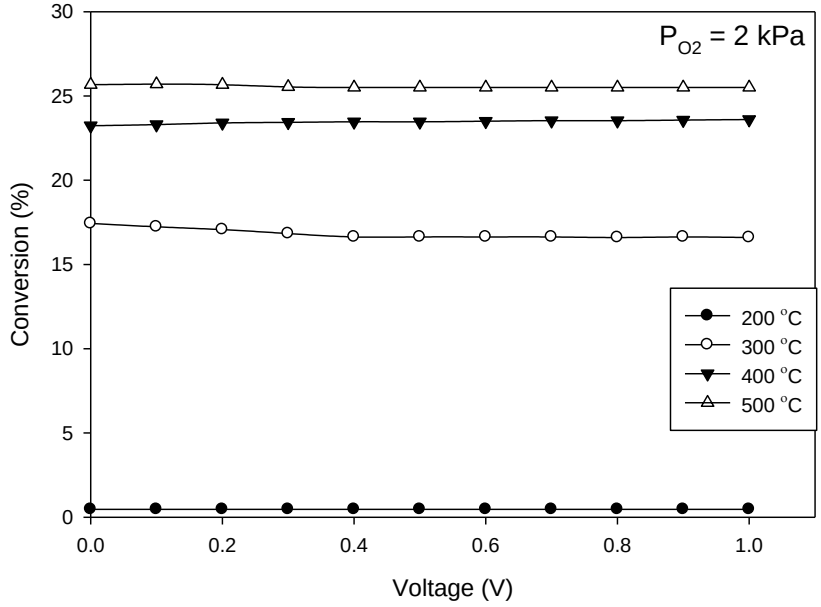
P$_{O2}$ = 2 kPa
Conversion (%)
Voltage (V)
200 °C
300 °C
400 °C
500 °C

(c)

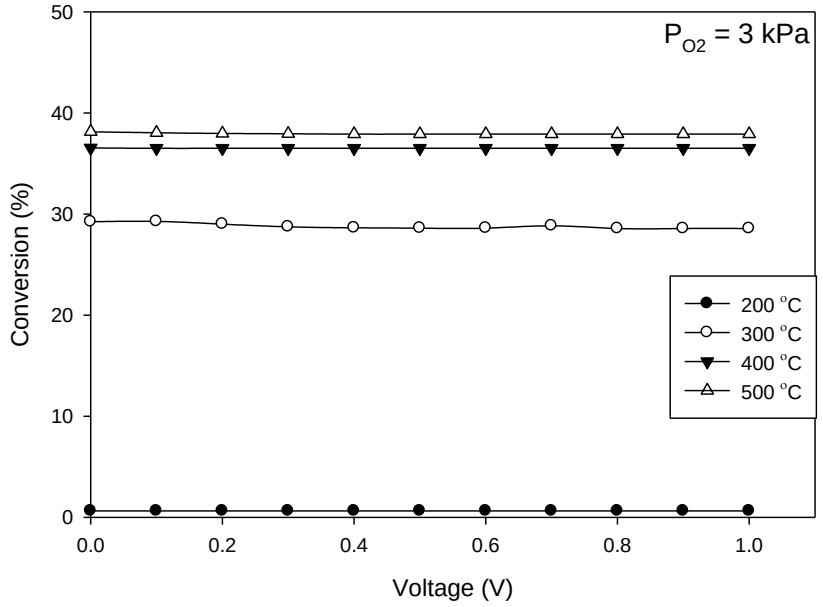
P_{O2} = 3 kPa
Conversion (%)
Voltage (V)
200 °C
300 °C
400 °C
500 °C
0
10
20
30
40
50
0.0
0.2
0.4
0.6
0.8
1.0

(d)

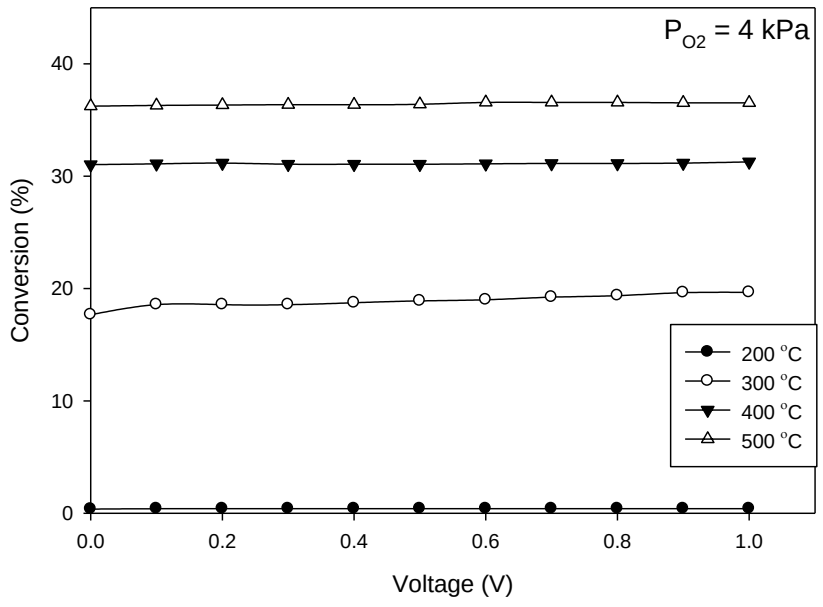
P_{O2} = 4 kPa
Conversion (%)
Voltage (V)
200 °C
300 °C
400 °C
500 °C
0
10
20
30
40
0.0
0.2
0.4
0.6
0.8
1.0

(e)

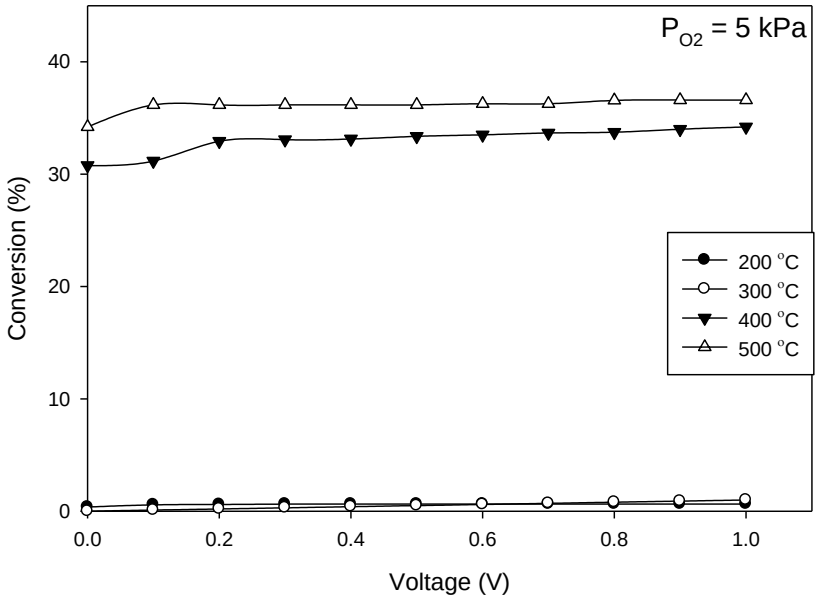

Figure 4.2.14 Propane conversions obtained when currents were applied on Pt electrochemical catalyst at temperature range of 200-500 ℃ with various P_{O2} (a) 1 kPa, (b) 2 kPa, (c) 3 kPa, (d) 4 kPa and (e) 5 kPa at P_{C3H8} 1 kPa.

According to Figure 4.2.14, it can be seen that the percentages of propane conversion were significantly increased as the temperature increased. Propane conversion slightly increased at partial pressure 4 and 5 kPa at the range of temperature from 200 to 500 ℃ and increased at partial pressure of oxygen 1 kPa at high temperature (400 and 500 ℃). It was found that the temperature and partial pressure influenced the propane conversion more than the applied voltage. These results agree with the effects on rate of carbon dioxide (Figure 4.2.14).

CHAPTER V
CONCLUSIONS AND RECOMMENDATIONS

5.1 Conclusions

The electrochemical catalytic oxidation reaction of propane on wireless configuration of impregnation and sputtered Pt electrode on YSZ disks were studied under open-circuit and closed-circuit conditions and difference temperature. The highest Faradaic efficiency was found at 200 °C, 5 V for wet impregnation method of 0.11 mgPt/m^2 (WI1) and 200 °C, 3 V for sputtering method of 0.26 mgPt/m^2 (SP2). At temperature greater than 200 °C, the results did not show NEMCA effect.

The electrochemical catalytic oxidation reaction of propane on Pt-sputtered film on YSZ disks were studied under open-circuit and closed-circuit conditions. The cell operating at closed-circuit, the reaction at oxygen partial pressure of 4 and 5 kPa, under near stoichiometric feed condition, at the range of temperature from 200 to 500 °C exhibited NEMCA effects of the electrophobic behavior, i.e. rate increase by positive potential application. In general, the reaction at oxygen partial pressure of 1, 2 and 3 kPa exhibited NEMCA effects of the electrophilic behavior, i.e. rate decrease by positive potential application. The maximum Faradaic efficiency and rate ratio reach value up to 2.5×10^5 and 1.7 found at 200 °C, 5 kPa of P_{O2} and 0.1 V.

5.2 Recommendations

1. Use other preparation method for metallic films to investigate the NEMCA effect.

2. Study the Pt loading by sputtering method in conventional configuration by spending sputtering time less than 45 min.

3. Use Electrostatic Force Microscopy (EFM) techniques to measure electric properties on a sample surface of Pt metal on YSZ of wireless configuration for description about the irreversible faradaic efficiency values.

REFERENCES

[1] *Deactivation Correlations Of Pd/Rh Three-Way Catalysts Designed For Euro IV Emission Limits*. 2003.

[2] Kokkofitis, C., and Stoukides, M., *Rate and oxygen activity oscillations during propane oxidation on Pt/YSZ.* Journal of Catalysis, 2006. **243**: p. 428–437.

[3] Kokkofitis, C., Karagiannakis, G., Zisekas, S., and Stoukides, M., *Catalytic study and electrochemical promotion of propane oxidation on Pt/YSZ.* Journal of Catalysis, 2005. **234**: p. 476–487.

[4] Group, T.F., *CATALYST PREPARATION Science and Engineering*. 2007.

[5] *Supported Metals in Catalysis*. 2 ed, ed. G.I. Hutchings. Vol. 11.

[6] Depla, D., Mahieu, S. and Greene, J.E. *Sputter deposition processes*. 1-36.

[7] Balonek, G., *Coating a Grating Structure Using Various Deposition Techniques*.

[8] Bultela, L., Vernouxb, P., Gaillardb, F., Rouxa, C., and Siebert, E., *Electrochemical and catalytic properties of porous Pt–YSZ composites.* Solid State Ionics, 2005. **176**: p. 793–801.

[9] Penga, Z., Liua, M., and Balko, Ed., *A new type of amperometric oxygen sensor based on a mixed-conducting composite membrane.* Sensors and Actuators B, 2001. **72**: p. 35-40.

[10] Shiga H., O.T., and Sadakata M., *Preparation of Nanostructured Platinum/Yttria-Stabilized Zirconia Cermet by the Sol-Gel Method.* Ind. Eng. Chem. Res., 1996. **35**: p. 4479-4486.

[11] Todorovska, R., Petrova, N., and Todorovsky, D., *Spray pyrolysis deposition of YSZ and YSZ–Pt composite films.* Applied Surface Science, 2005. **252**: p. 1266–1275.

[12] Souentie, S., Lizarraga, a, L., Papaioannou, E.I., Vayenas, C.G., and Vernoux, P., *Permanent electrochemical promotion of C3H8 oxidation over thin sputtered Pt films.* Electrochemistry Communications, 2010. **12**: p. 1133-1135.

[13] Lizarragaa, L., Gutha, M., Billard b, A., and Vernouxa, P., *Electrochemical catalysis for propane combustion using nanometric sputtered-deposited Pt films.* Catalysis Today, 2010. **157**: p. 61-65.

[14] Kotsionopoulos, N., and Bebelis, S., *Electrochemical promotion of the oxidation of propane on Pt/YSZ and Rh/YSZ catalyst-electrodes.* Journal of Applied Electrochemistry, 2005. **35**: p. 1253–1264.

[15] ChaoYanga, X., XuChenb, L.,Yanb, Y., TiZhuangb, W., ZhiMina, Z., and SuPing, Y., *Preparation of nano-structured Pt–YSZ composite and its application in oxygen potentiometric sensor.* Applied Surface Science, 2011. **257**: p. 7952–7958.

[16] Billard, A., and Vernoux, P. , *Influence of the Thickness of Sputter-Deposited Platinum Films on the Electrochemical Promotion of Propane Combustion.* Ionics, 2005. **11**: p. 126-131.

[17] Koutsodontis, C., Katsaounis, A., Figueroa, J.C., Cavalca, C., Pereira, C.J., and Vayenas, C.G. , *The effect of catalyst film thickness on the magnitude of the electrochemical promotion of catalytic reactions.* Topics in Catalysis, 2006. **38**(1-3): p. 157-167.

[18] Koutsodontis, C., Katsaounis, A., Figueroa, J.C., Cavalca, C., Pereira, C., and Vayenasa, C.G., *The effect of catalyst film thickness on the electrochemical promotion of ethylene oxidation on Pt.* Topics in Catalysis, 2006. **39**(1-2): p. 97-100.

[19] Vayenas, C.G., Bebelis, S., Pliangos, C., Brosda, S., and Tsiplakides, D., *Electrochemical Activation of Catalysis Promotion, Electrochemical Promotion, and Metal-Support Interactions*. 2001.

[20] Vayenas, C.G., Brosda, S., and Pliangos, C., *Rules and Mathematical Modeling of Electrochemical and Chemical Promotion 1. Reaction Classification and Promotional Rules.* Journal of Catalysis, 2001. **203**(1): p. 329-350.

[21] Frantzis, A.D., Bebelis, S., and Vayenas, C.G. , *Electrochemical promotion (NEMCA) of CH4 and C2H4 oxidation on Pd/YSZ and investigation of the origin of NEMCA via AC impedance spectroscopy.* Solid State Ionics, 2000. **136–137**: p. 863–872.

[22] Roche V., K.R., Billard A., Revel R., and Vernoux P., *Electrochemical promotion of deep oxidation of methane on Pd/YSZ.* J Appl Electrochem, 2008. **38**: p. 1111-1119.

[23] Mateia, F., Ciuparua, D., Jiménez-Borjab, C., Doradob, F., Valverdeb J.L., and Brosda S. , *Electrochemical promotion of methane oxidation on impregnated and sputtered Pd catalyst-electrodes deposited on YSZ.* Applied Catalysis B: Environmental, 2012. **127**: p. 18-27.

[24] Jiménez-Borja, C., Brosda, S., Matei, F., Makri, M., Delgado, B., Sapountzi,F. Ciuparu, D., Dorado, F., Valverdea, J.L., and Vayenas, C.G., *Electrochemical promotion of methane oxidation on Pd catalyst-electrodes deposited on Y2O3-stabilized-ZrO2.* Applied Catalysis B: Environmental, 2012. **128**: p. 48-54.

[25] Matei, F., Jiménez-Borja, C., Canales-Vázquez, J., Brosda, S., Dorado, F., Valverde, J.L., and Ciuparu, D., *Enhanced electropromotion of methane combustion on palladium catalysts deposited on highly porous supports.* Applied Catalysis B: Environmental, 2013. **132-133**: p. 80-89.

[26] Kokkofitis, C., Karagiannakis, G., and Michael, S., *Electrochemical promotion in O2) cells during propane oxidation.* 2007. **44**(3).

[27] Bebelis, S., and Kotsionopoulos, N., *Non-faradaic electrochemical modification of the catalytic activity for propane combustion of Pt/YSZ and Rh/YSZ catalyst-electrodes.* Solid State Ionics, 2006. **177**: p. 2205–2209.

[28] Tsampas, M.N., Sapountzi, F.M., Boréave A., Vernoux P., *Isotopical labeling mechanistic studies of electrochemical promotion of propane combustion on Pt/YSZ.* Electrochemistry Communications, 2013. **26**: p. 13-16.

[29] Vernoux, P., Gaillard, F., Bultel, L., Siebert, E., and Primet M., *Electrochemical Promotion of Propane and Propene Oxidation on Pt/YSZ.* Journal of Catalysis, 2002. **208**: p. 412–421.

[30] Beatricea, P., Pliangosb, C., Worrella, W.L., and Vayenas, C.G., *Electrochemical promotion of ethylene and propylene oxidation on Pt deposited on yttria–titania–zirconia.* Solid State Ionics, 2000. **136–137**: p. 833–837.

[31] Nicole, J., and Comninellis, Ch., *Electrochemical promotion of oxide catalyst for the gas phase combustion of ethylene.* Solid State Ionics, 2000. **136–137**: p. 687–692.

[32] Pliangos, C., Yentekakis, I.V., Ladas, S., and Vayenas, C.G., *Non-Faradaic Electrochemical Modification of Catalytic Activity 9. Ethylene Oxidation on Pt Deposited on TiO2.* JOURNAL OF CATALYSIS, 1996. **159**: p. 189-203.

[33] de Lucas-Consuegra, A., Dorado, F., Luis Valverde, J., Karoum, R., and Vernoux, P. , *Electrochemical activation of Pt catalyst by potassium for low temperature CO deep oxidation.* Catalysis Communications, 2008. **9**: p. 17-20.

[34] Xia, C., Falgairette, C., Li, Y., Foti, G., Comninellis, C., and Harbich, W., *Electrochemical promotion of CO combustion over Pt/YSZ under high vacuum conditions.* Applied Catalysis B: Environmental, 2012. **113-114**: p. 250-254.

[35] B6guin, B., Gaillard, F., Primet, M., Vernoux, P., Bultel, L., H~nault, M., Roux, C., and Siebert, E., *Electrochemical Promotion of NO Reduction by Propene on Pt/YSZ.* |onics, 2002. **2**: p. 128-135.

[36] Brosda, S., and Vayenas, C.G., *Rules and Mathematical Modeling of Electrochemical and Classical Promotio 2. Modeling.* Journal of Catalysis, 2002 **208**(2): p. 38-53.

[37] Tsampas, M.N., and Vernoux, P., *Electrochemical Promotion of Catalysis for Automotive Post-Treatment and Air Cleaning*, in *Catalysis for Remediation and Environmental Concerns*. 2013.

[38] *NOTE Electrochemical Promotion of Electronically Isolated Pt Catalysts on Stabilized Zirconia.* Journal Of Catalysis, 1997. **168**: p. 538-542.

[39] Balomenou S., P., G., Polydoros, D., Giannikos A., Vradis, A., Frenzel, A., Pliangosa, C., Pu¨tterc, H., and Vayenas, C.G. , *Electrochemical promotion of Pd, Fe and distributed Pt catalyst-electrodes.* Solid State Ionics, 2000. **136-137**: p. 857-862.

[40] Pliangos, C., Raptis, C., Bolzonella I., Comninellis, Ch., and Vayenas, C.G. , *Electrochemical Promotion of Conventional and Bipolar Reactor Configurations for NO Reduction.* 2002: p. 372-382.

[41] Poulidi, D., Mather, G.C., and Metcalfe, I.S., *Wireless electrochemical modification of catalytic activity on a mixed protonic–electronic conductor.* Solid State Ionics, 2007. **178**: p. 675–680.

[42] Poulidi, D., and Metcalfe, I.S., *In situ catalyst activity control in a novel membrane reactor — Reaction driven wireless electrochemical promotion of catalysis.* Chemical Engineering Science, 2010. **65**: p. 446-450.

[43] Kiilunen, M., Aitio, A., and Santonen, T., *Chapter 50 Platinum*, in *Handbook on the Toxicology of Metals 4E*. 2015. p. 1125-1141.

[44] Aitio, A., Kiilunen, M., Santonen, T., and Nordberg, M., *Chapter 38 Gold and Gold Mining*, in *Handbook on the Toxicology of Metals 4E*. 2015. p. 817-843.

[45] Vernoux, P., Lizarraga, L., Tsampas, M.N., Sapountzi, F.M., De Lucas-Consuegra, A., Valverde, J., Souentie, S., Vayenas, C.G., Tsiplakides, D., Balomenou, S., and Baranova, E.A. , *Ionically Conducting Ceramics as Active Catalyst Supports.* Chemical Reviews, 2013.

[46] Derek Fray, A.V., and Mounsey, S., *Electrolyte*. www.doitpoms.ac.uk/tlplib/fuel-cells/printall.php.

[47] *Electrolyte*, in *Science and technology of ceramic fuel cells*. 1995. p. 69-116.

[48] Miller, J.T., Schreier, M., Jeremy Kropf A., and Regalbuto, J.R., *A fundamental study of platinum tetraammine impregnation of silica 2. The effect of method of preparation, loading, and calcination temperature on (reduced) particle size.* Journal of Catalysis, 2004. **225**: p. 203-212.

[49] Davis, M.E. and R.J. Davis, *Fundamentals of chemical reaction engineering*. 2012: Courier Corporation.

APPENDIX

APPENDIX A

CALIBRATION OF PLATINUM LOADING

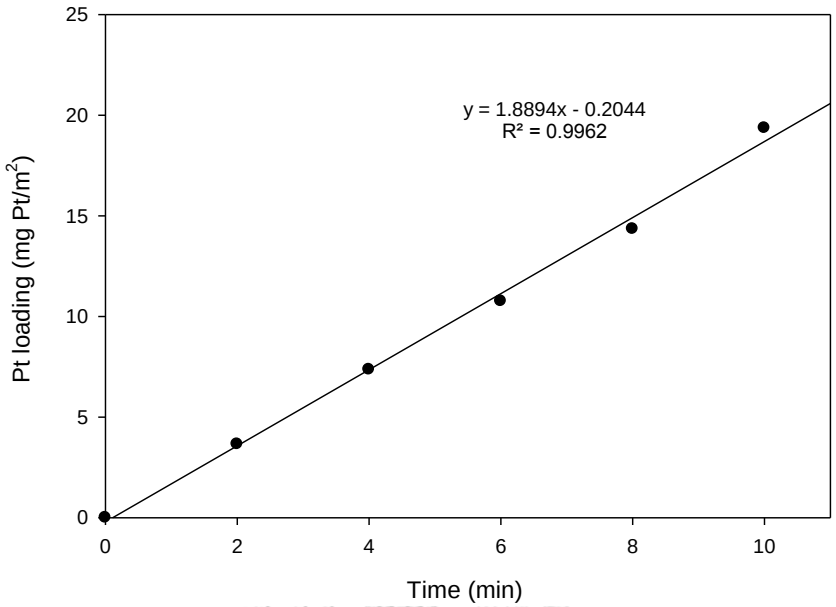

Figure A1 Calibration curve from ICP technique plot between Pt loading (mg Pt/m^2) and sputtering time (min)

For example, calculate platinum loading per area (mg Pt/m^2):

Pt loading (mgPt/ m^2) = 1.8894 (45 min) – 0.2044

Therefore, Pt loading = 84.82 mgPt/ m^2

APPENDIX B

CALIBRATION OF REACTANT GAS FLOW RATE

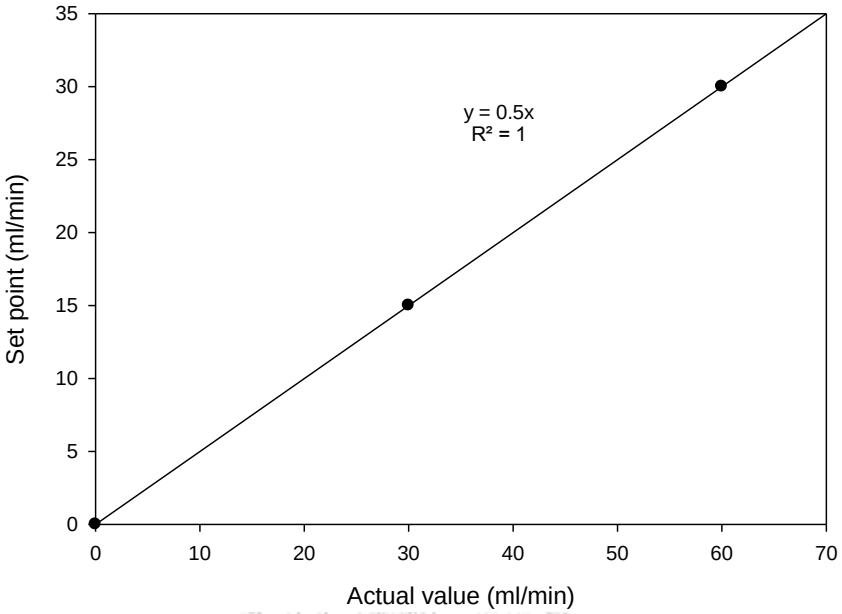

Figure B1 Calibration curve of oxygen volumetric flow rate.

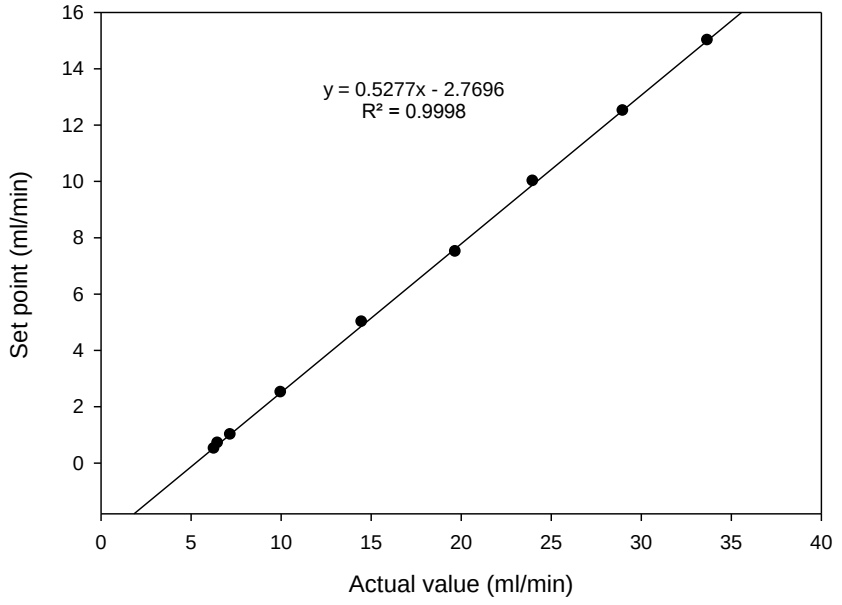

Figure B2 Calibration curve of propane volumetric flow rate.

APPENDIX C
CALCULATION FOR THE RATE ENHANCEMENT RATIO AND FARADAIC EFFICIENCY

Propane oxidation: $C_3H_8 + 5O_2 \longrightarrow 3CO_2 + 4H_2O$

Electrochemical propane oxidation: $C_3H_8 + 10O^{2-} \longrightarrow 20e- + 3CO_2 + 4H_2O$

The rate enhancement ratio, ρ

$$\rho = r/r^{\circ}$$

Where r° = the catalytic rate at open circuit

r = the electrochemically promoted catalytic rate

The Faradaic efficiency, Λ

$$\Lambda = (r-r^{\circ})/ (I/nF)$$

Where I = the applied current

F = Faraday's constant (96,485 C/mol)

n = the charge of the promotion ion

For example,

Reactant gas feed: C_3H_8 = 50.0 cm^3/ min,

O^2 = 33.33 cm^3/ min,

He = 16.67 cm^3/ min

The CO^2 concentration of blank YSZ (no platinum) obtained 0.033 vol%

Under open circuit;

CO^2 concentration = 1.059 vol%

Under closed circuit;

Current = 6.65×10^{-6} A. (C.s-1), Voltage = 0.1 V,

Temperature = 500 °C, P_{O2} = 5 kPa and P_{C3H8} = 1 kPa

CO^2 concentration = 1.118 vol%

Find the rate under closed circuit:

$$r = \frac{1}{3} \times \frac{\frac{1.118-0.033}{100} \times (50+33.33+16.67)\text{cm}^3\text{min}^{-1} \times \frac{1\text{min}}{60\text{ sec}} \times 10^5\text{Pa}}{8314000\ \text{cm}^3\text{PaK}^{-1}\text{mol}^{-1} \times (30+273.15)\text{K}}$$

$r = 2.3916 \times 10^{-7}$ mol s^{-1}

Find the rate under open circuit:

$$r^{\circ} = \frac{1}{3} \times \frac{\frac{1.059-0.033}{100} \times (50+33.33+66.67)\text{cm}^3\text{min}^{-1} \times \frac{1\text{min}}{60\text{ sec}} \times 10^5\text{Pa}}{8314000\ \text{cm}^3\text{PaK}^{-1}\text{mol}^{-1} \times (30+273.15)\text{K}}$$

$r^{\circ} = 2.2615 \times 10^{-7}$ mol s^{-1}

Find the rate enhancement ratio from $\rho = \frac{r}{r^o}$

$$= \frac{2.3916 \times 10^{-7}\ \text{mol}\ s^{-1}}{2.2615 \times 10^{-7}\ \text{mol}\ s^{-1}}$$

Therefore $\rho = 1.06$

And, find the Faradaic efficiency from $\Lambda = \frac{(r-r^{\circ})}{(I/nF)}$

$$= \frac{(2.3916 \times 10^{-7} - 2.2615 \times 10^{-7})\ \text{mol}\ s^{-1}}{\frac{6.65 \times 10^{-6}\ \text{C}\ s^{-1}}{20 \times 96{,}485\ \text{C}\ \text{mol}^{-1}}}$$

Therefore $\Lambda = 3772.83$

Data of the effects of voltage on faradaic efficiency at various temperatures and partial pressure of oxygen

(a)

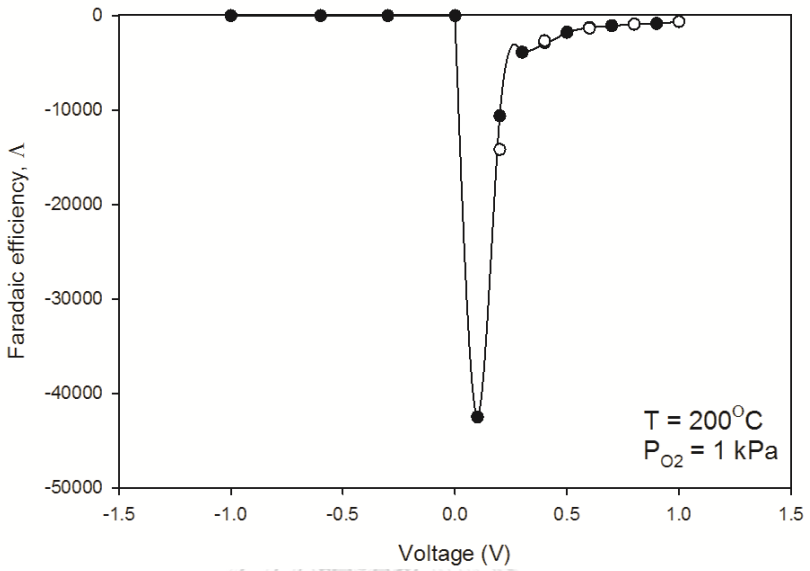

(b)

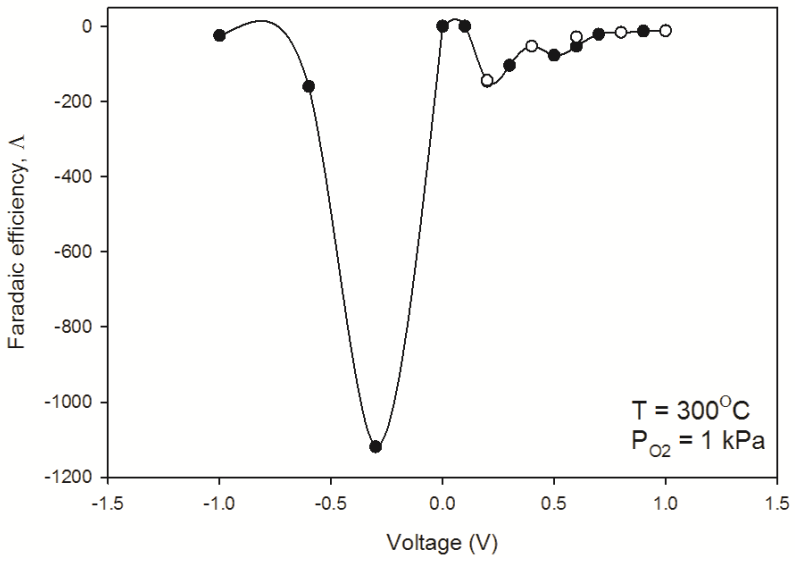

(c)

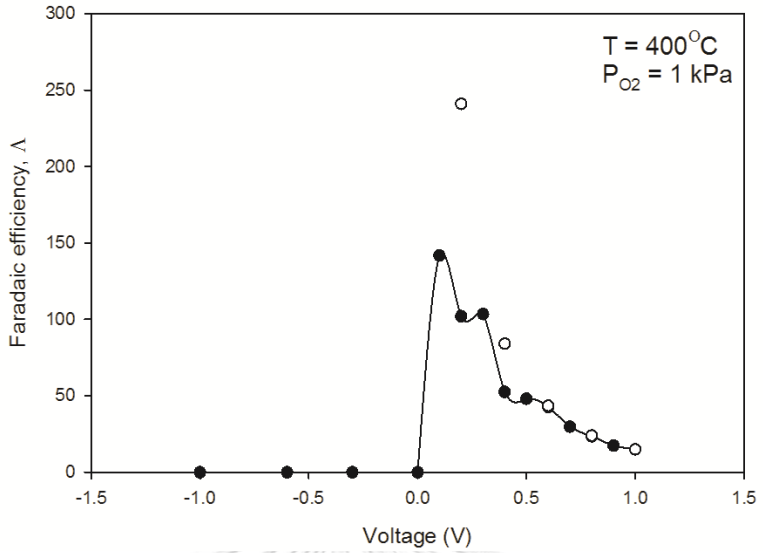

(d)

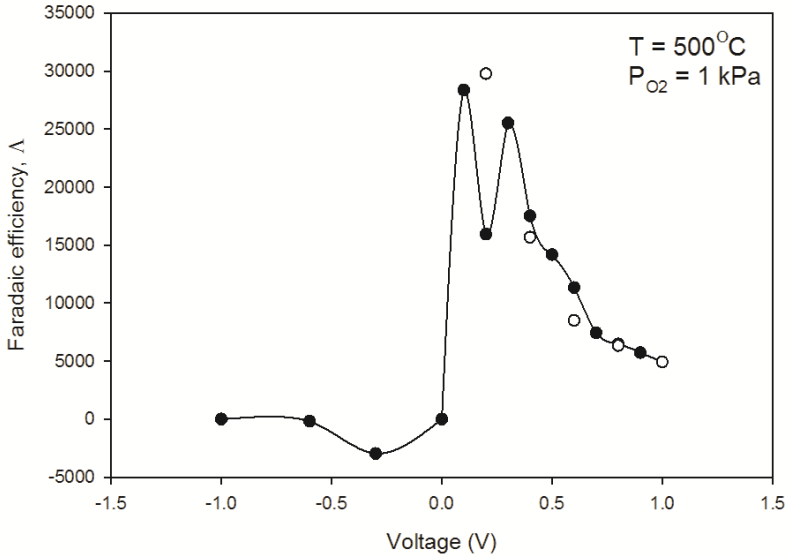

Figure C1 Dependence of Faradaic efficiency on voltage (V) at partial pressure of propane P_{C3H8} 1 kPa and oxygen P_{O2} 1 kPa and temperature (a) 200 °C (b) 300 °C (c) 400 °C and 500 °C (reversible value, ○)

(a)

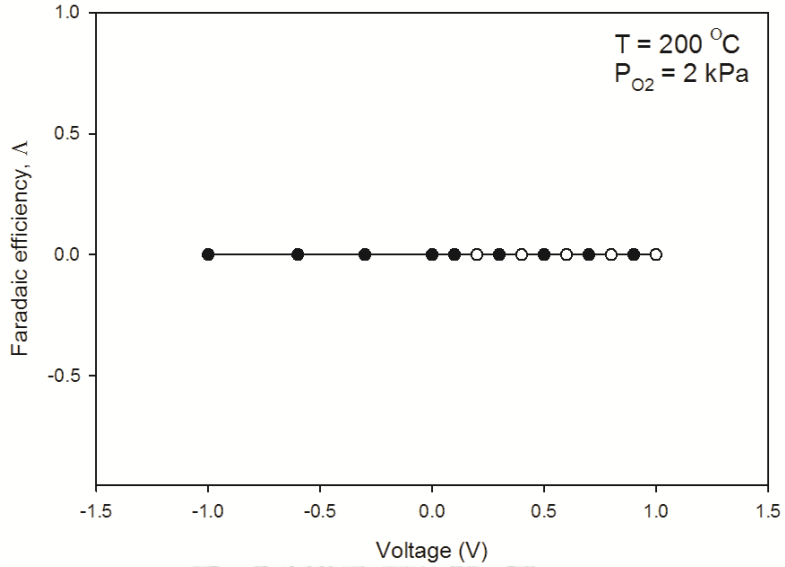
T = 200 °C
P_{O2} = 2 kPa
Faradaic efficiency, Λ
Voltage (V)
1.0
0.5
0.0
-0.5
-1.5
-1.0
-0.5
0.0
0.5
1.0
1.5

(b)

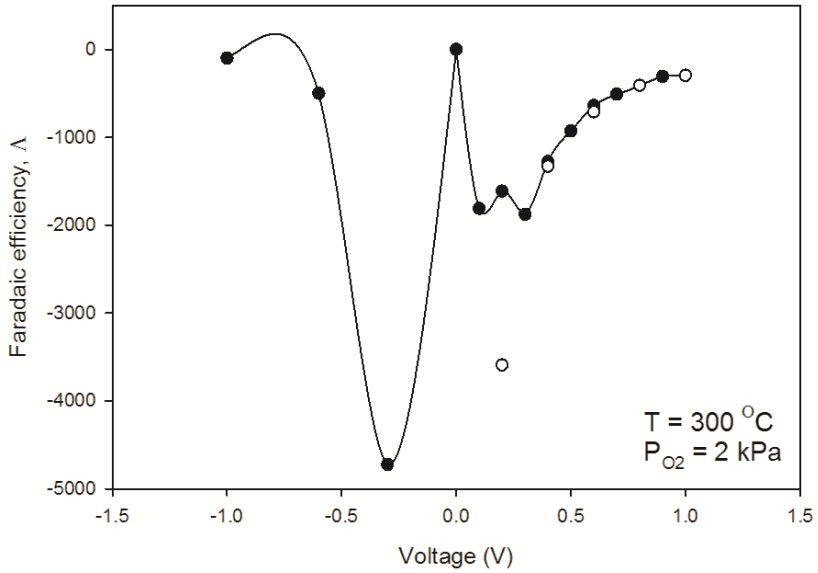
T = 300 °C
P_{O2} = 2 kPa
Faradaic efficiency, Λ
Voltage (V)
0
-1000
-2000
-3000
-4000
-5000
-1.5
-1.0
-0.5
0.0
0.5
1.0
1.5

(c)

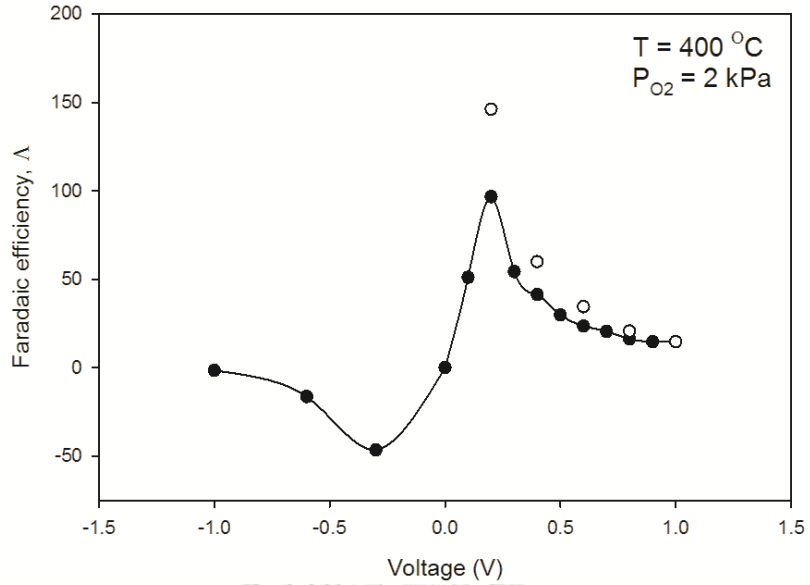

(d)

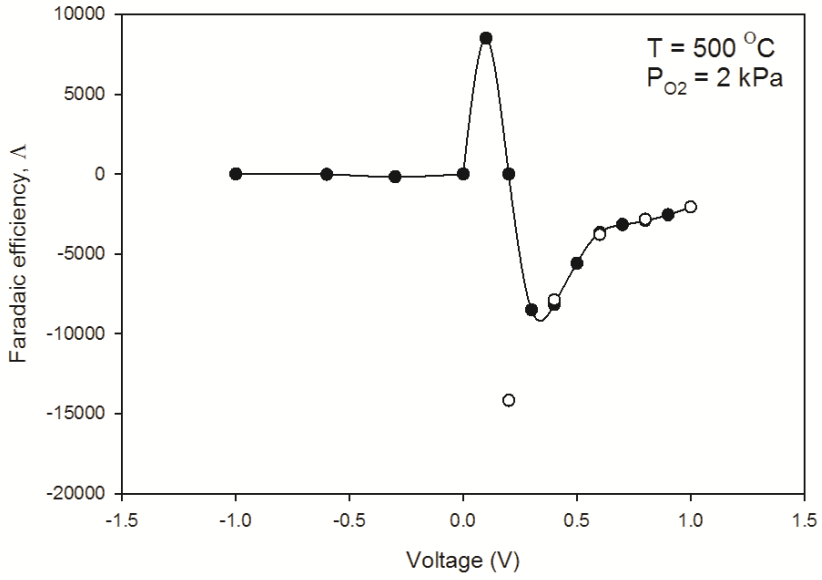

Figure C2 Dependence of Faradaic efficiency on voltage (V) at partial pressure of propane P_{C3H8} 1 kPa and oxygen P_{O2} 2 kPa and temperature (a) 200 °C (b) 300 °C (c) 400 °C and 500 °C (reversible value, ○)

(a)

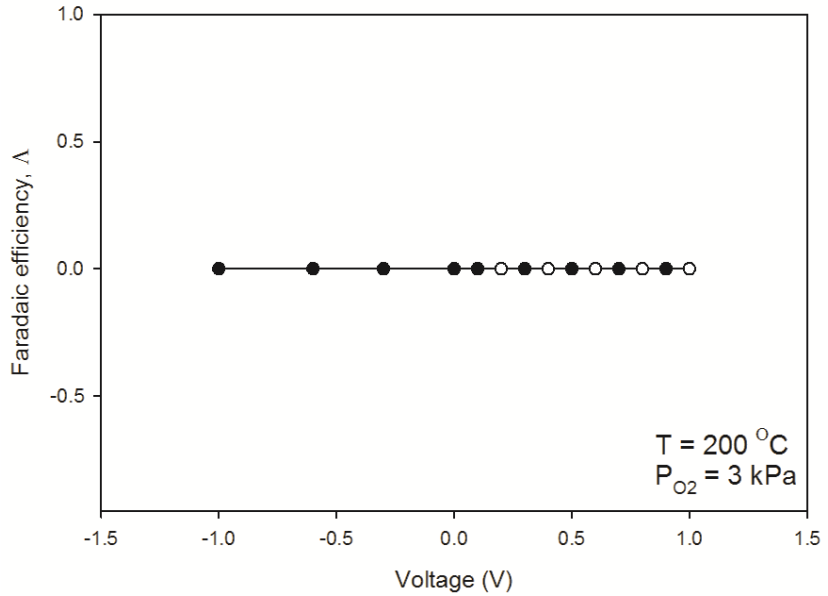
1.0
0.5
0.0
-0.5
Faradaic efficiency, Λ
T = 200 °C
P$_{O2}$ = 3 kPa
-1.5
-1.0
-0.5
0.0
0.5
1.0
1.5
Voltage (V)

(b)

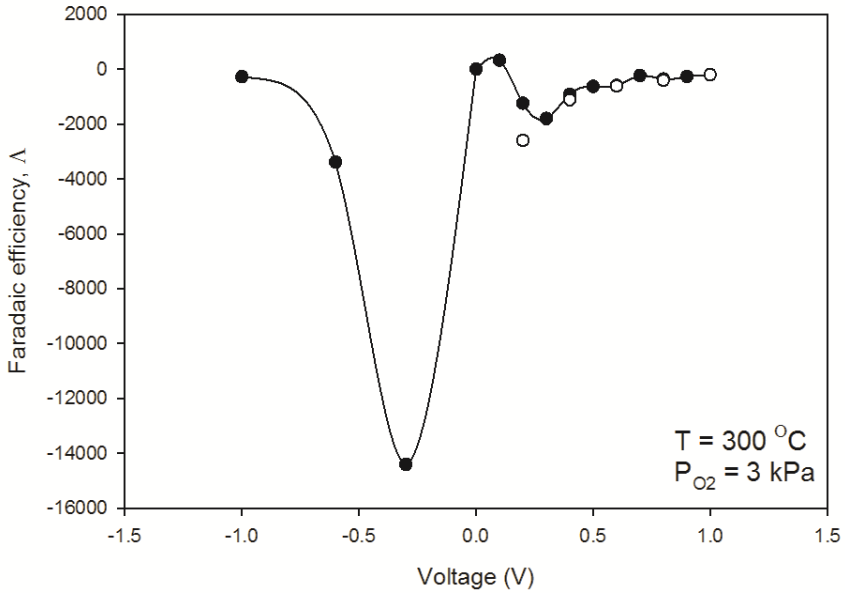
2000
0
-2000
-4000
-6000
-8000
-10000
-12000
-14000
-16000
Faradaic efficiency, Λ
T = 300 °C
P$_{O2}$ = 3 kPa
-1.5
-1.0
-0.5
0.0
0.5
1.0
1.5
Voltage (V)

(c)

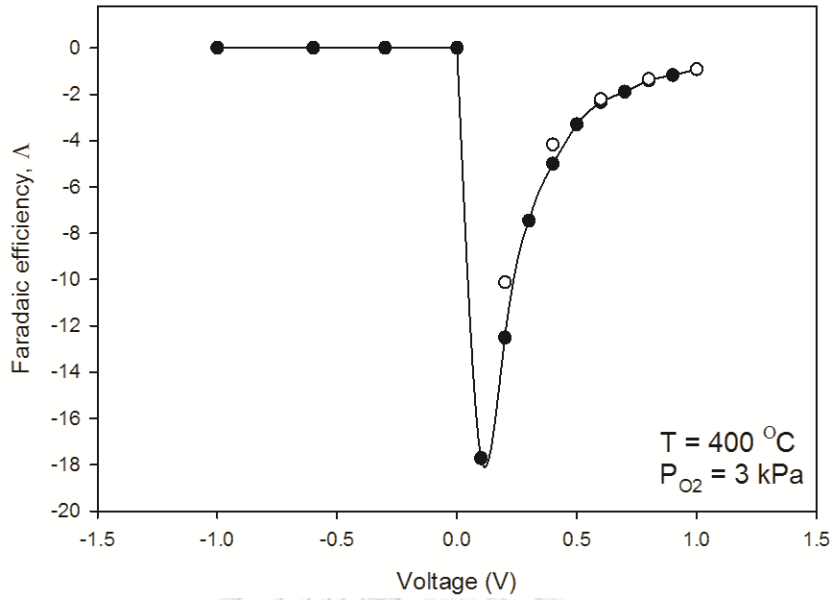

(d)

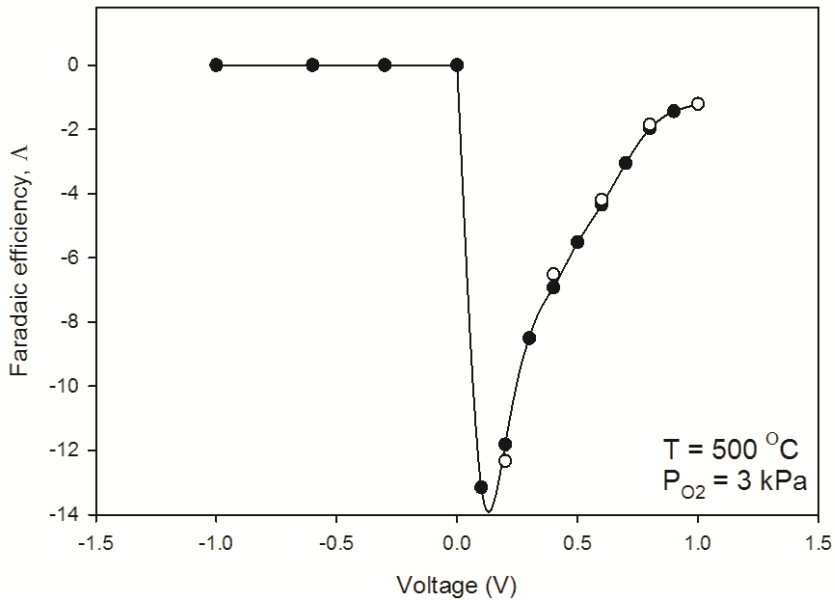

Figure C3 Dependence of Faradaic efficiency on voltage (V) at partial pressure of propane P_{C3H8} 1 kPa and oxygen P_{O2} 3 kPa and temperature (a) 200 °C (b) 300 °C (c) 400 °C and 500 °C (reversible value, ○)

(a)

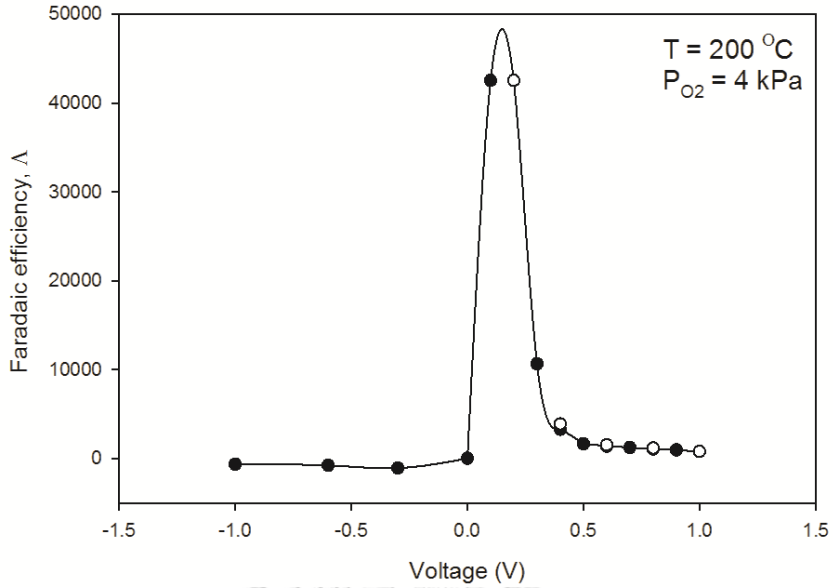
T = 200 °C
P_{O2} = 4 kPa
Faradaic efficiency, Λ
Voltage (V)
50000
40000
30000
20000
10000
0
-1.5
-1.0
-0.5
0.0
0.5
1.0
1.5

(b)

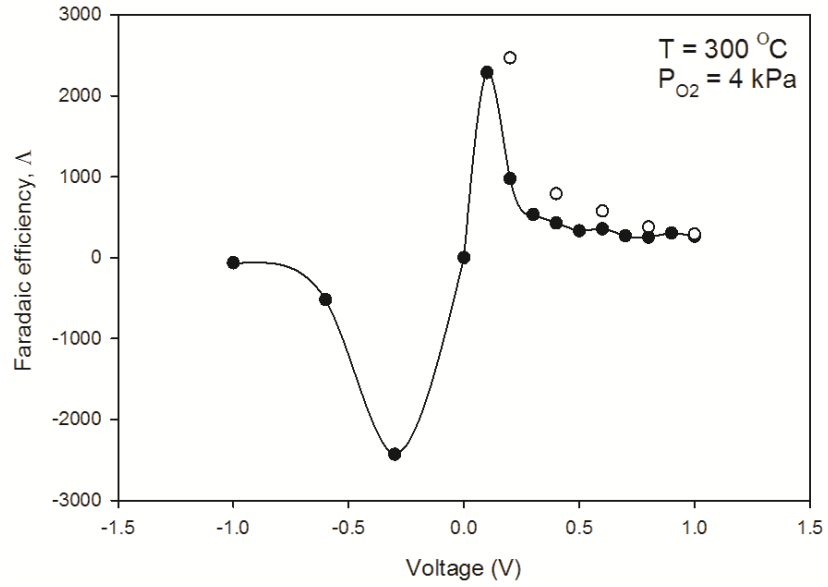
T = 300 °C
P_{O2} = 4 kPa
Faradaic efficiency, Λ
Voltage (V)
3000
2000
1000
0
-1000
-2000
-3000
-1.5
-1.0
-0.5
0.0
0.5
1.0
1.5

(c)

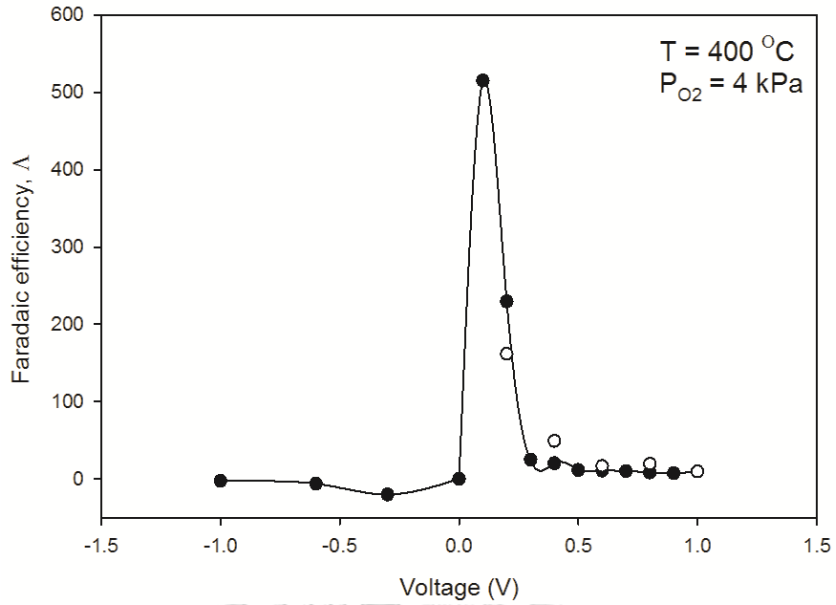

(d)

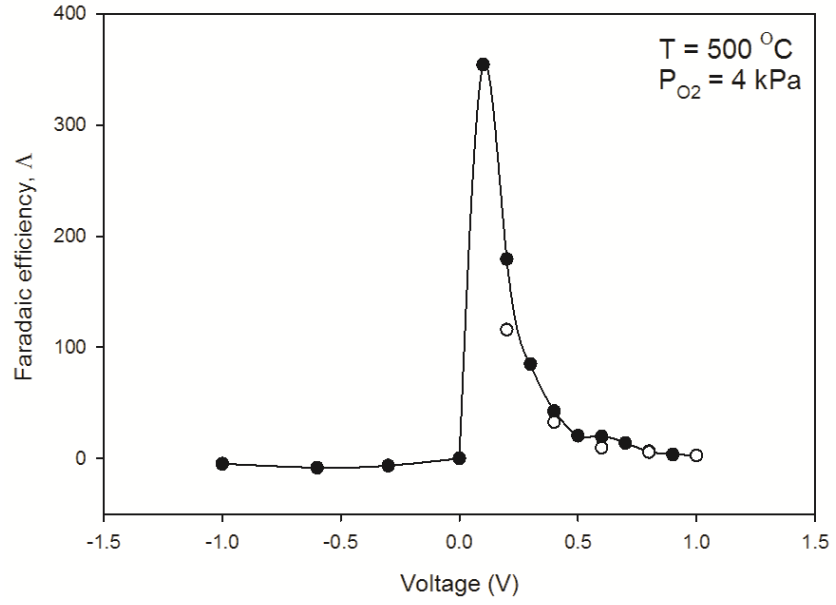

Figure C4 Dependence of Faradaic efficiency on voltage (V) at partial pressure of propane P_{C3H8} 1 kPa and oxygen P_{O2} 4 kPa and temperature (a) 200 ℃ (b) 300 ℃ (c) 400 ℃ and 500 ℃ (reversible value, ○)

(a)

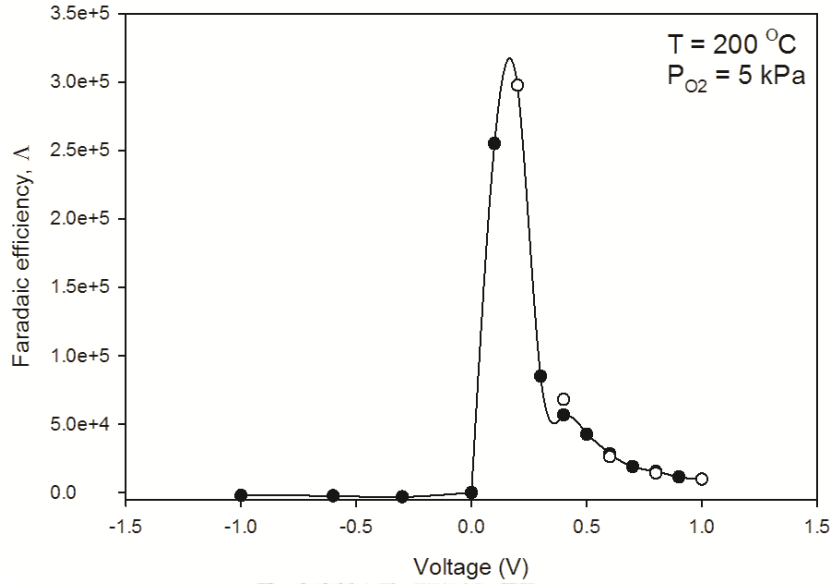
T = 200 °C
P$_{O2}$ = 5 kPa
Faradaic efficiency, Λ
3.5e+5
3.0e+5
2.5e+5
2.0e+5
1.5e+5
1.0e+5
5.0e+4
0.0
-1.5
-1.0
-0.5
0.0
0.5
1.0
1.5
Voltage (V)

(b)

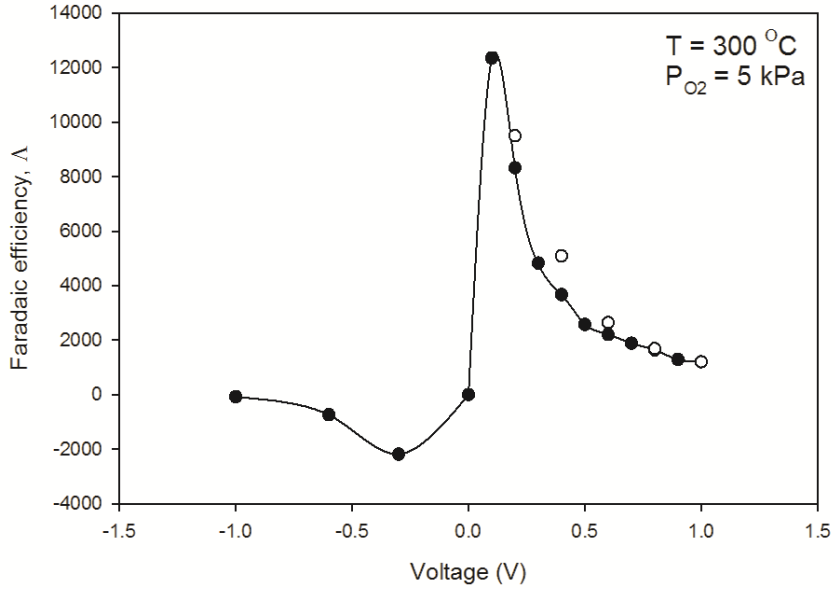
T = 300 °C
P$_{O2}$ = 5 kPa
Faradaic efficiency, Λ
14000
12000
10000
8000
6000
4000
2000
0
-2000
-4000
-1.5
-1.0
-0.5
0.0
0.5
1.0
1.5
Voltage (V)

(c)

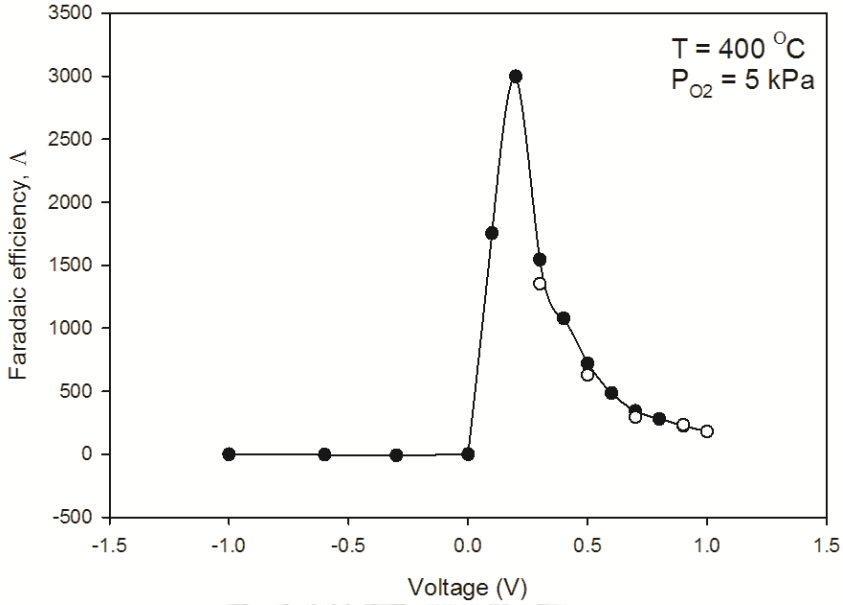

(d)

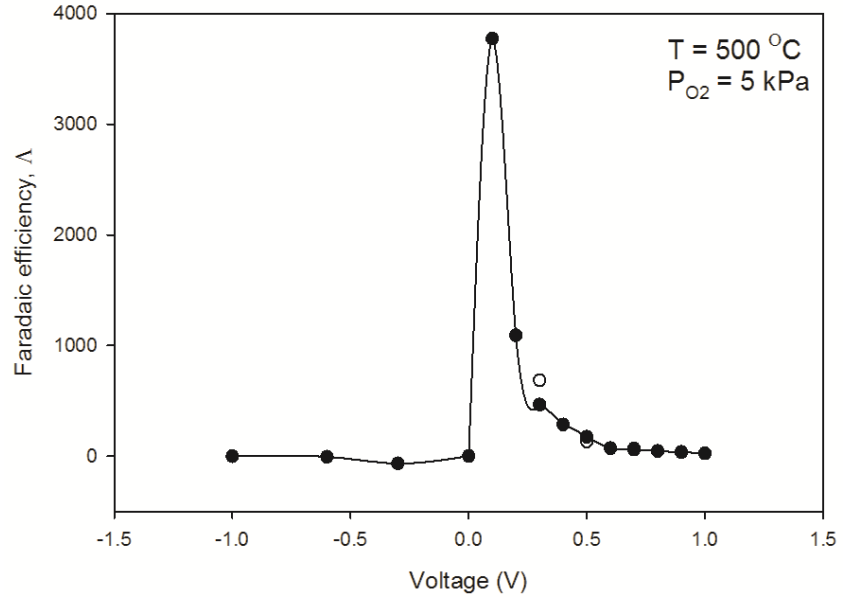

Figure C5 Dependence of Faradaic efficiency on voltage (V) at partial pressure of propane P_{C3H8} 1 kPa and oxygen P_{O2} 5 kPa and temperature (a) 200 °C (b) 300 °C (c) 400 °C and 500 °C (reversible value, ○)

APPENDIX D

CALCULATION FOR PROPANE CONVERSION

Propane oxidation: $C_3H_8 + 5O_2 \longrightarrow 3CO_2 + 4H_2O$

The propane conversion was followed as;

$$\%\text{Conversions} = \frac{\mathbf{P_{CO2}}}{\mathbf{P_{CO2}+3P_{C3H8}}} \times 100\%$$

Where P_{CO2} are the carbon dioxide partial pressures

P_{C3H8} are the outlet propane partial pressures

For example,

Voltage = 0.1 V, Temperature = 500 °C, P_{O2} = 5 kPa

CO^2 concentration of blank YSZ (no platinum) = 0.033 vol%

Inlet P_{C3H8} = 1 kPa

Outlet CO^2 concentration = 1.118 vol%

$$\%\text{conversions} = \frac{\mathbf{1.118-0.033}}{\mathbf{(1.118-0.033)+(3\times(1-(\frac{1.118-0.033}{3})))}} \times 100\%$$

%conversions = **36.17 %**